

A DETAILED STUDY OF THE EMISSION LINES IN THE SEYFERT 1 NUCLEUS OF M81

ALEXEI V. FILIPPENKO¹

Department of Astronomy, University of California, Berkeley

AND

WALLACE L. W. SARGENT

Palomar Observatory, California Institute of Technology

Received 1987 May 11; accepted 1987 June 22

ABSTRACT

We present optical spectra of M81 having moderate resolution (1.6–4.5 Å) and exceptionally high signal-to-noise ratios ($S/N \gtrsim 100/1$). The broad component of $H\alpha$ emission first noticed by Peimbert and Torres-Peimbert is easily visible, confirming that M81 harbors an active galactic nucleus (AGN) of the Seyfert 1 type. Prominent forbidden lines are also present, but many features are severely contaminated by the underlying starlight. An absorption-line template galaxy, NGC 4339, is used to eliminate the stars, revealing the pure emission-line spectrum of M81.

After carefully removing the narrow component of $H\alpha$ and the neighboring $[N\ II] \lambda\lambda 6548, 6583$ lines, we measure full widths at half-maximum (FWHM) and near zero intensity (FWZI) of 2200 and 6900 km s^{-1} , respectively, for the broad $H\alpha$ emission line. Its absolute luminosity, uncorrected for extinction, is 1.2×10^{39} ergs s^{-1} . This is ~ 0.05 of the broad $H\alpha$ in the faintest known classical Seyfert 1 nucleus, NGC 4051. We derive $L_X/L_{H\alpha} \approx 23$, well within the range observed in classical broad-line AGNs. Extrapolation of the observed X-ray spectrum to longer wavelengths fails to provide enough ionizing photons to account for the emission lines.

In addition to the broad component of $H\alpha$ emission, the data convincingly show the corresponding component of $H\beta$ (FWHM $\approx 1800 \text{ km s}^{-1}$; FWZI $\approx 5800 \text{ km s}^{-1}$). The intensity ratio of broad $H\alpha$ to $H\beta$ is ~ 6.6 , rather than the recombination ratio of ~ 3 . If reddening is the sole reason for the discrepancy, an extinction $A_V \approx 2$ mag is calculated, but the observed lower limit to the broad $H\gamma$ line gives a much smaller value ($A_V \lesssim 0.3$ mag). Under the assumption that the width of $H\beta$ is produced by clouds in Keplerian orbits, the mass interior to the broad-line region ($r = 0.0013\text{--}0.0036$ pc) is calculated to be $3\text{--}8 \times 10^5 M_\odot$. A single central object, presumably a black hole, probably accounts for most of this mass.

Comparison of spectra obtained over several days, 1 month, 1 yr, and 3 yr reveals no variations in the strength or the shape of the broad $H\alpha$ emission line. Given its low luminosity, this is quite puzzling; the Balmer lines of other, brighter type 1 Seyferts are known to vary substantially. Moreover, at X-ray energies M81 has brightened by factors of 3–5 over the past 7 yr, and it has exhibited X-ray variability of a factor of 2 in 600 s. The rapid X-ray fluctuations may be produced by broad-line clouds moving across our line of sight to the continuum source.

The forbidden lines in M81 exhibit a strong correlation between profile width and critical density. $[O\ I] \lambda 6300$, for example, is far broader than each of the $[S\ II] \lambda\lambda 6716, 6731$ lines. This implies that the narrow-line region (NLR) of M81 is composed of clouds having a wide range of electron densities ($n_e \approx 10^{2.5}\text{--}10^{7.5} \text{ cm}^{-3}$). The densest clouds are optically thick, have the highest bulk motions, and live closest to the nucleus. Additional support for this interpretation is found from an analysis of the individual $[S\ II]$ lines themselves: $[S\ II] \lambda 6716$ is noticeably narrower than $[S\ II] \lambda 6731$, whose critical density is a factor of 2.6 larger. The relative intensity of the two lines actually reaches the high-density limit ($n_e \gtrsim 10^5 \text{ cm}^{-3}$) in the extreme wings, which are produced by high-velocity gas.

High densities and large optical depths in the NLR alleviate several previous problems with photoionization models of LINERs. The electron temperature is low, rather than high, in the O^{++} zone, and the great strength of $[O\ I] \lambda 6300$ is easily explained. Some of these results are inconsistent with the hypothesis that shock heating is the dominant excitation mechanism in the NLR of M81. This supports the conclusion that the LINERs found in many galaxies may be genuine, albeit low-luminosity, AGNs in which gas is photoionized by a nonstellar continuum.

Subject headings: galaxies: individual — galaxies: nuclei — galaxies: Seyfert — line profiles — spectrophotometry

¹ Guest Observer, Palomar Observatory, which is owned and operated by the California Institute of Technology.

I. INTRODUCTION

The very bright ($B_T = 7.86$ mag), nearby ($d \approx 3.3$ Mpc; Sandage and Tammann 1975) Sb(r)I-II galaxy M81 (NGC 3031) has been the subject of numerous investigations. Münch (1959) noted that the nuclear region ($r \lesssim 2''.5$) exhibits prominent, relatively narrow emission lines, and a more detailed analysis (Peimbert 1968) suggested that the very large intensity ratio of [N II] $\lambda 6583$ to $H\alpha$ is at least partially due to an overabundance of N relative to O. High ratios of [N II]/ $H\alpha$ had also been found in other galactic nuclei (Burbidge and Burbidge 1962, 1965), but the cause was somewhat controversial. As discussed by Heckman (1980), the overall spectrum of M81 is that of "low-ionization nuclear emission-line regions" (LINERs), whose characteristics he attributed to heating by shocks (e.g., Shull and McKee 1979). Heckman (1980) also presented evidence that not all of the narrow lines have the same width in M81.

While investigating the ultraviolet (UV) and optical spectrum of M81, Peimbert and Torres-Peimbert (1981; hereafter referred to as PTP) discovered a broad component of $H\alpha$ emission (FWZI ≈ 5300 km s $^{-1}$) blended with the narrower component and the neighboring [N II] $\lambda\lambda 6548, 6583$ lines. Broad $H\alpha$ was independently noticed by Shuder and Osterbrock (1981), making M81 the nearest, least luminous known Seyfert 1 nucleus. PTP also reported the presence of broad components of $H\beta$ and Mg II $\lambda 2800$ emission, although in our opinion the former is not visible in their published spectra.

Studies of M81 at other energies further revealed its active nucleus. A bright, compact, flat-spectrum radio source was found by van der Kruit (1973). It is variable by a factor of 50% over 5 days at 8 GHz (Crane, Giuffrida, and Carlson 1976; see also de Bruyn *et al.* 1976), suggesting that the source size is $\lesssim 10^{16}$ cm. Interferometry with very long baselines (Kellermann *et al.* 1976) shows that the source is unresolved ($< 0''.0004$) at 5 GHz, confirming the size estimate quoted above. It is $\sim 10^4$ times stronger than Sgr A West. The radiation is presumably of synchrotron origin, and exhibits a cutoff near 7 GHz.

Elvis and Van Speybroeck (1982; hereafter EVS) used the High Resolution Imager (HRI) aboard *Einstein Observatory* to discover an unresolved, soft X-ray source of luminosity 1.7×10^{40} ergs s $^{-1}$ (energy range 0.5–4.5 keV) coincident with the optical and radio nucleus. Hard X-rays were also detected from M81. Barr and Giommi (1985) reported *EXOSAT* observations which showed that the soft and hard X-ray fluxes had increased by factors of 5 and 3, respectively, over the previous *Einstein* values, and that the source can vary by up to 50% over $\lesssim 1$ hr. During one observation, changes of a factor of 2 were seen in only 600 s (Barr *et al.* 1985)! This suggests that the X-ray emission is produced in the vicinity of a single, massive, compact object, rather than by binary stars in the nuclear region, although its steep spectrum ($f_\nu \propto \nu^{-1.4}$; EVS) is unusual for Seyfert galaxies (Rothschild *et al.* 1983). A non-stellar continuum has never been firmly detected at optical and UV wavelengths.

M81 is included in the spectroscopic survey of 500 bright, northern galaxies we are conducting at Palomar Observatory. Spectra having extremely high S/N ratios confirm the presence of broad $H\alpha$ emission (Filippenko and Sargent 1985, 1986; hereafter referred to as Papers I and II), as well as large differences in the widths and profiles of the forbidden lines. In fact, the overall properties of the narrow emission lines resemble those of several previously studied LINERs and low-

luminosity Seyfert 1 galaxies that are well explained by photoionization models.

The potential importance of M81 for our general understanding of the AGN phenomenon is very great. Its activity appears to be similar to, but much weaker than, that in classical QSOs, and the currently achievable spatial resolution is unprecedented. This prompted us to observe M81 extensively, paying special attention to the profiles of different emission lines and to possible variations in the broad $H\alpha$ flux. This is the first of two articles in which the results of our work are presented in detail. Some of our conclusions have already been described in portions of various conference proceedings (Filippenko and Sargent 1987*a, b*; Filippenko 1987; hereafter referred to as Papers III, IV, and V, respectively). A few of the measured quantities reported here differ slightly from, and supersede, those quoted previously.

We begin by documenting our observations and reductions of M81. Section III describes the subtraction of the underlying stellar continuum, outlines the procedures used to measure the emission lines, and discusses reddening. Some comments are also made concerning the nonstellar continuum and the X-ray flux. A detailed analysis of the NLR follows (§ IV). We show that a wide range of densities is present, making the observed relative intensities consistent with photoionization by dilute, nonstellar radiation. In § V we derive the mass of the central object in M81 ($M \approx 5 \times 10^5 M_\odot$), under the assumption that the widths of the broad permitted lines are induced by gravity. Section VI illustrates that there appear to have been no changes in the strength of the broad $H\alpha$ line during the past few years, even though the X-ray flux of M81 has been observed to vary substantially. A possible cause of very rapid X-ray variability is discussed. Our main conclusions are summarized in § VII.

II. OBSERVATIONS AND REDUCTIONS

M81 was observed on many occasions during the past few years with the Double Spectrograph (Oke and Gunn 1982) at the Cassegrain focus of the Hale 5.08 m reflector at Palomar Observatory (see Table 1). A long slit of width $2''$ was generally used at a position angle (P.A.) of 65° , close to the parallactic angle at the time of the first observation on 1984 February 12 UT. This simplified comparisons between the strengths of emission lines, some of which arise from spatially extended regions. The approximate wavelength ranges $\lambda\lambda 4220\text{--}5090$ (blue camera, 600 groove mm $^{-1}$ grating, first order) and $\lambda\lambda 6210\text{--}6860$ (red camera, 1200 groove mm $^{-1}$ grating, first order) were observed simultaneously, with resolutions (FWHM) of 4.0–4.5 Å and 2.0–2.6 Å, respectively. A dichroic filter directly behind the slit split the light beam at ~ 5500 Å. Texas Instruments charge-coupled devices (TI CCDs) were employed to record all of the two-dimensional data discussed in this paper. A few spectra were also taken through a $4''$ slit, to provide accurate fluxes in the nuclear region. Typical S/N ratios per resolution element are $\gtrsim 100/1$.

On one night (1986 February 25 UT), we procured spectra at six different position angles with a slit width of $1''$. The main purpose of these observations was to study the rotation curve and ionization gradients in M81, and the results will be reported elsewhere. Data from the 1500 s integration obtained just as M81 was crossing the meridian, however, will be used extensively in this paper, since much less starlight was included than with a $2''$ slit. During this observation, the slit was placed at the parallactic angle of 180° to minimize the effects of atmospheric

TABLE 1
JOURNAL OF PALOMAR OBSERVATIONS: M81

UT Date	Start	Exposure (s)	P.A. ^a	P.P.A. ^b	Width ^c	Air Mass ^d	Seeing ^e	Weather
1984 Feb 12	04:52	600	65°	63°	2"	1.41	2"-2.3	Cloudy
1984 Feb 12	05:07	1500	65	57	2	1.37	2-2.3	Cloudy ^f
1986 Feb 18	05:20	950	45	47	2	1.32	3-4	Cloudy
1986 Feb 25	04:19	600	60	57	4	1.37	2-3	Clear
1986 Feb 25	06:59	1500	180	182	1	1.23	1-1.5	Clear
1986 Feb 25	07:32	1000	138 ^g	172	1	1.24	1-1.3	Clear
1986 Feb 25	07:52	1100	48 ^h	165	1	1.24	1-1.5	Clear
1986 Feb 25	08:13	400	65	160	2	1.25	1-1.5	Clear
1986 Feb 25	08:22	1100	90	154	1	1.26	1-1.3	Clear
1986 Mar 27	02:59	300	65	47	2	1.32	0.8-1	Clear
1986 Mar 27	03:07	300	45	45	4	1.31	0.8-1	Clear
1986 Mar 29	05:49	960	65	164	2	1.24	1-1.3	Cloudy
1987 Jan 24	09:46	400	65	171	2	1.24	1.5	Clear
1987 Feb 22	05:02	600	65	49	2	1.33	1.5	Cloudy
1987 Feb 22	05:16	1200	65	43	2	1.30	1.5-2	Cloudy

^a Actual position angle of slit, through nucleus.

^b Parallaxic position angle, midpoint of exposure.

^c Slit width. Usable slit length $\approx 100''$.

^d Defined as secant of zenith angle at midpoint of exposure.

^e Visually estimated seeing disk.

^f Many halts due to clouds.

^g Approximate major axis of M81.

^h Approximate minor axis of M81.

dispersion (Filippenko 1982). The spectral resolution in the blue camera was 2.1–2.5 Å, except near the blue end, where it flared up to more than 4 Å because of a warp in the CCD. Similarly, the resolution was 1.6–1.7 Å in the red camera, except blueward of $\sim \lambda 6400$, where it steadily increased from 2 Å to 3 Å.

We followed standard procedures when reducing the data (Papers I and II; Djorgovski and Spinrad 1983). Cosmic rays, a bias level, local variations in pixel sensitivity, and geometric distortions were removed from each two-dimensional spectrum. The background sky, chosen to be at least 46'' from the nucleus, included small contributions from starlight and emission-line gas in M81, but our final results are essentially unaffected by this. One-dimensional spectra of the nucleus were subsequently extracted by summing over the central 7 pixels of the red CCD (0'.58 pixel⁻¹), and the central 10 pixels of the blue CCD (0'.40 pixel⁻¹). Thus, the effective apertures were $\sim 1'' \times 4''$, $2'' \times 4''$, or $4'' \times 4''$, where the first dimension represents the slit width used. Such long apertures were chosen because the focus varies substantially along the uneven, tilted surface of each CCD, making accurate relative intensities exceedingly difficult to derive from spectra consisting of only a small number (≤ 4) of pixels along the slit. Of course, this means that the contribution of starlight is quite large in the final spectra, making measurements of faint emission lines more uncertain, but at least the *systematic* errors are minimized.²

Spectra of bright secondary standard stars (Oke and Gunn 1983) were obtained to calibrate relative and absolute fluxes.

² This is one of the very few situations in which observations made through an aperture of fixed size can, in some respects, be superior to those obtained with a long slit and a two-dimensional detector. If the object is nearly overhead, so that atmospheric dispersion is negligible, a small aperture (e.g., $1'' \times 1''$) may be used to isolate light of all colors from the nucleus alone, excluding much of the surrounding starlight. Of course, photometrically accurate one-dimensional spectra can easily be extracted from individual rows of a two-dimensional spectrum obtained with a CCD whose surface is very flat and coincident with the focal plane.

The slit was always aligned along the parallactic angle, and the effective apertures used in the two-dimensional extractions were the same as those for the galaxy spectra. Thus, the fluxes derived for point sources were absolute if guiding errors and the atmospheric seeing did not vary during the night. This technique obviously overestimates the fluxes of extended objects, with the maximum error occurring for objects having constant surface brightness. The nucleus of M81, however, is semistellar, and the seeing was roughly constant during many of the observations. Our procedure should therefore provide reasonably accurate absolute fluxes, especially for the broad permitted lines, which presumably originate in a spatially unresolved region. Imperfect guiding is probably the major source of error, but it is difficult to quantify.

Division of each spectrum of M81 by normalized, intrinsically featureless spectra of the bright standard stars adequately removed telluric oxygen absorption lines near $\lambda 6860$ (the B band) and $\lambda 6280$. A few other, much weaker, telluric features may still remain, since this procedure was followed only around the wavelengths quoted above. All data were corrected for continuum atmospheric extinction in the usual manner.

Spectra of He, Ne, Ar, and Fe were used to determine the wavelength scales. In general, a cubic or quartic polynomial proved to be an excellent fit to the observed positions of emission lines, with typical residuals (1σ) being $\sim 5\%$ of the instrumental resolution. The arc spectra also provided a quantitative measure of the spectral resolution as a function of position on the CCDs. This was useful when the intrinsic widths of emission lines in M81 were being determined.

III. ANALYSIS OF THE SPECTRA

a) Subtraction of the Stellar Continuum

Figure 1a illustrates the red spectrum of M81 obtained on 1986 February 25 UT. As described in § II, it represents the light through a rectangular aperture ($1'' \times 4''$; P.A. = 180°), and was synthesized from the two-dimensional data. The helio-

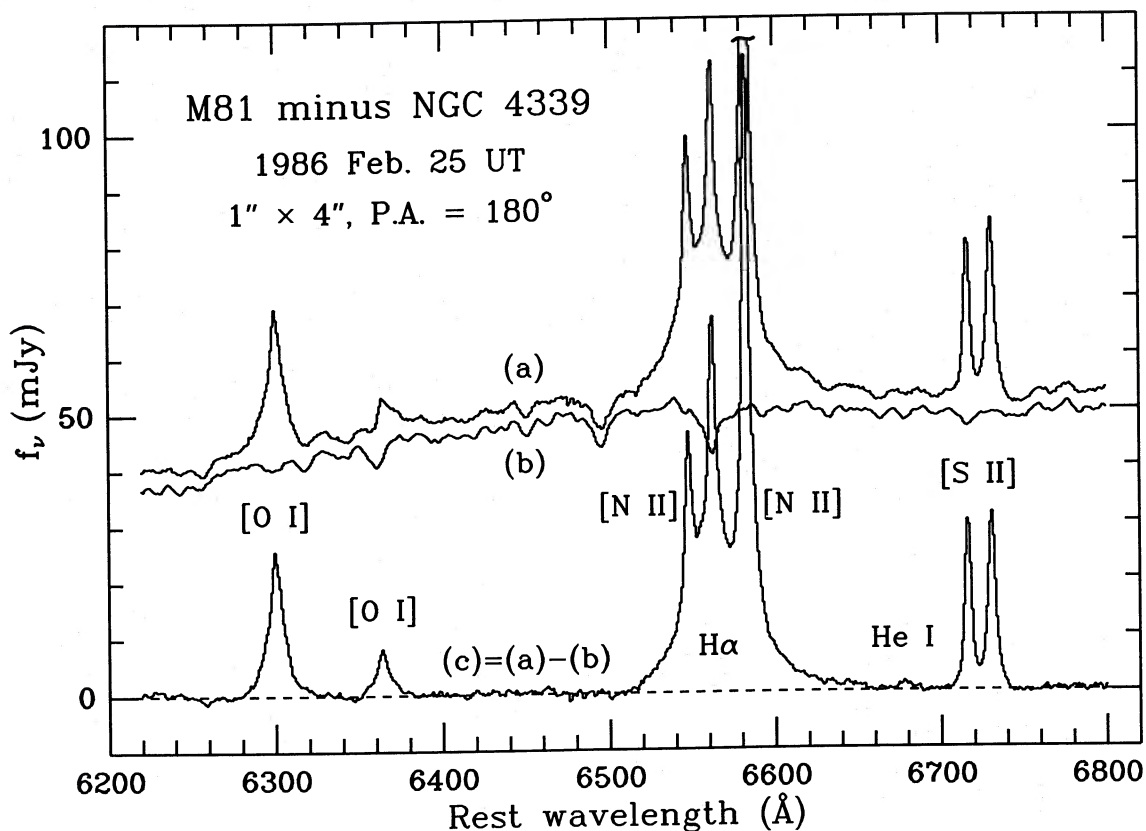


FIG. 1.—(a) Flux-calibrated red spectrum of M81, obtained through an effective entrance aperture of $1'' \times 4''$ centered on the nucleus. The data have not been smoothed. Note the broad component of H α emission, as well as the markedly different widths and profiles of the [O I] and [S II] lines. (b) NGC 4339, an absorption-line template galaxy, is shown with an offset of -3 mJy for clarity. The spectrum has been scaled to match the flux density of M81. Spectrum (c) illustrates the difference between (a) and (b). [O I] $\lambda 6364$ is now relatively free from contamination by absorption lines, as are He I $\lambda 6678$, the very extended red wing of H α , and several other features. [S II] $\lambda 6731$ is significantly broader than [S II] $\lambda 6716$.

centric velocity of M81 ($v = -28$ km s $^{-1}$), determined from the observed wavelengths of the peaks of narrow emission lines in six of our spectra, has been removed. Comparison with two previously published spectra (Papers I and II) reveals the remarkably high quality of the data; very few differences are detectable. Strong, broad H α emission is visible, and forbidden lines of different ions exhibit dissimilar profiles in some cases.

A major obstacle to the accurate measurement of emission lines is the underlying starlight. Regions between strong absorption lines can mimic emission features, and the absorption lines themselves often hide or greatly diminish weak emission lines. This has been shown explicitly by Koski and Osterbrock (1978), Keel and Miller (1983), Filippenko and Halpern (1984; hereafter FH84), Rose and Tripicco (1984), Filippenko (1985a; hereafter F85), and many others, especially in the context of NGC 1052, the prototypical LINER. It is necessary to eliminate the starlight by subtraction of an appropriate absorption-line template. Here we use spectra of other galactic nuclei as templates, although one could also employ off-nuclear spectra of the same galaxy (e.g., PTP) or construct a template from spectra of various bright stars (Keel 1983). Many template spectra are available from our extensive spectroscopic survey of bright galaxies (Paper I).

A spectrum of the S0 $_{1/2}$ (0) galaxy NGC 4339 (Sandage and Tammann 1981), which lacks emission lines, is shown in Figure 1b. It was obtained with the same instrument as the M81 data. The metallicity and velocity dispersion in the nuclei

of NGC 4339 and M81 are nearly identical; we modified the spectrum of NGC 4339 only slightly by convolving it with a Gaussian function having a FWHM of 2 Å. In addition, a quadratic polynomial having very little curvature was fitted to the ratio of the two spectra and was subsequently multiplied by the spectrum of NGC 4339. Since regions devoid of emission lines were used exclusively in the least-squares fit, this procedure removed slight differences in the overall shapes of the continua (caused, for example, by different internal or Galactic reddening), and forced the spectrum of NGC 4339 to have the same continuum flux density as that of M81. It did *not*, however, introduce any high or moderate-frequency undulations which could be mistaken for broad emission lines like those in QSOs.

The adopted procedure precludes the discovery of any *non-stellar* contribution to the continuum in the wavelength regions being analyzed. Based on the strengths of the emission lines, such a continuum is expected to be weak (§ III d), making its detection very difficult anyway. The dispersion in the equivalent widths of absorption lines in galactic nuclei is so large that it effectively masks the dilution produced by a featureless, nonstellar continuum whose intensity is only a few percent that of starlight. Perhaps we could detect such a continuum in a statistical manner by comparing the strengths of absorption lines in many galactic nuclei lacking emission lines with the corresponding strengths in emission-line nuclei. This would best be done at $\lambda \lesssim 4000$ Å, where absorption lines in normal

stars have large equivalent widths. Also, the nonstellar continuum is more readily detected at UV and blue wavelengths (e.g., F85; Koski 1978) owing to the smaller contribution of starlight (see also § III*d*).

The pure emission-line spectrum of M81, which we obtained by subtracting the spectrum of NGC 4339 from that of M81, is shown in Figure 1*c*. It is clear that the troublesome absorption lines have been removed with high accuracy. Only a few minor spurious features, such as those at 6260 Å and 6462 Å, are present. The small bump at 6678 Å is larger than both of these, and it also falls exactly at the laboratory wavelength of He I λ 6678. This, together with the fact that its observed relative strength is comparable to that of He I λ 6678 in typical AGNs, makes its reality unquestionable. Another line which was heavily contaminated prior to the subtraction is [O I] λ 6364. Its measured intensity is 0.27 that of [O I] λ 6300, not quite the theoretically expected value (0.33), but the strength of [O I] λ 6300 may have been overestimated because of contamination by [S III] λ 6312. [S II] λ 6716, which was originally superposed on Ca I λ 6718 absorption, is also affected slightly by the subtraction process.

The narrow H α emission line is stronger in Figure 1*c* than in Figure 1*a*, due to the removal of underlying H α absorption. Since a small excess of hot, young stars can substantially alter the observed strength of Balmer absorption lines in an otherwise old stellar population, the greatest uncertainty in the subtraction procedure described here occurs for the Balmer emission lines. The same problem exists with templates constructed out of many individual stellar spectra, or obtained

from locations far from galactic nuclei, and we cannot solve it without having spectra over the interval spanning the high-order Balmer lines. It is unlikely, however, that our measured strength of narrow H α is seriously in error; similar results were obtained when other galaxies were used as templates, and the bulge of M81 itself appears to consist of a normal, old stellar population. Galaxies such as NGC 404 (Paper II), having truly anomalous Balmer absorption-line strengths, are relatively rare.

Perhaps the most notable feature in Figure 1*c* is the broad component of H α emission, which shows that M81 does indeed harbor a low-luminosity Seyfert 1 nucleus. This line, first reported by PTP and confirmed by Shuder and Osterbrock (1981), is easily visible in spectra published two years earlier by Tonry and Davis (1979). Curiously enough, Heckman (1980) did not mention it in his extensive study of LINERs, even though he specifically searched for such a component in high-quality spectra of M81. This suggests that the line strength might be variable, although we conclude in § VI*b* that it is relatively constant. The broad component of H α in Figure 1*c* has FWZI \approx 6900 km s⁻¹ if one includes the very extended red half that can be traced almost to the He I λ 6678 line. This wing is present in all of our spectra of M81. Moreover, it persists when other galaxies are used as absorption-line templates, as well as when no corrections are made for slight differences in overall shapes of the stellar continua.

Figure 2 demonstrates the same procedure as in Figure 1, but for the blue spectral region of M81. Most of the emission lines in this region are weaker than those near H α , and the stellar

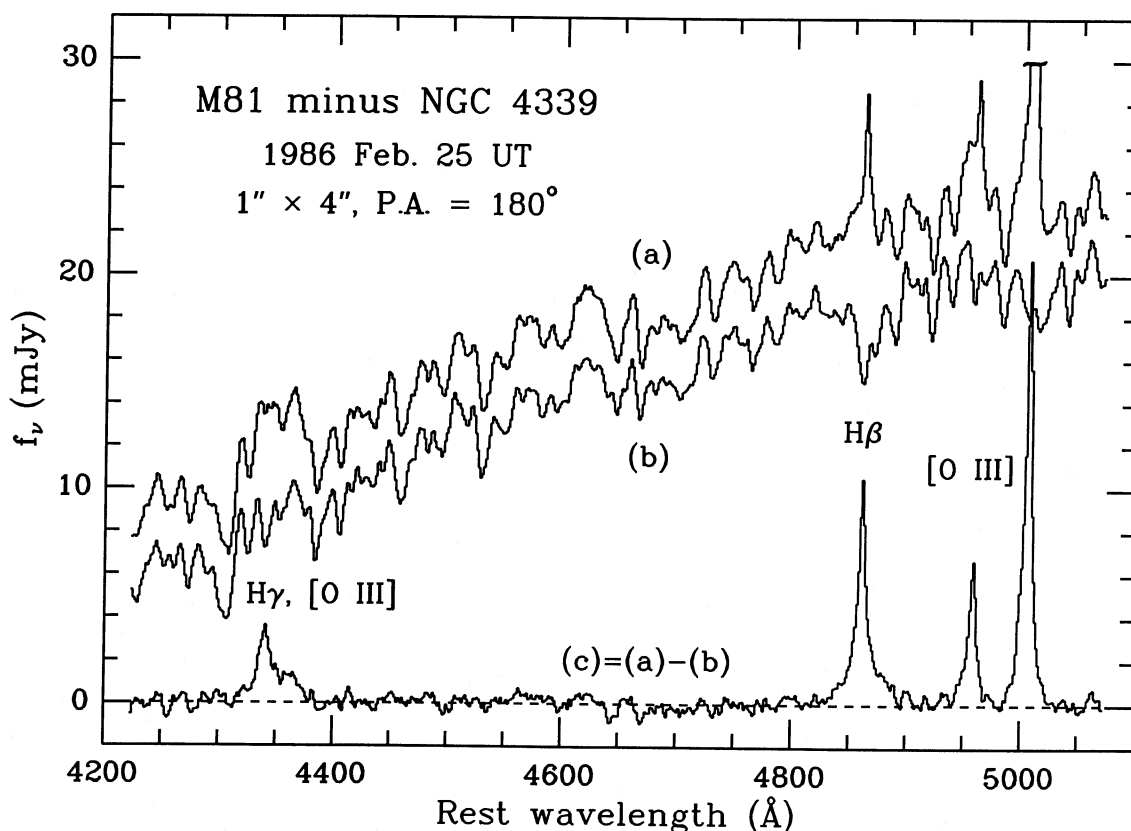


FIG. 2.—Same as Fig. 1, but for the blue spectral region of M81. Absorption lines from an old stellar population greatly affect the original spectrum (a), but these are removed with NGC 4339, as shown in (b) and (c). A broad component of H β emission (FWZI \approx 5800 km s⁻¹) is easily visible underneath the narrow component. Broad H γ contaminates [O III] λ 4363.

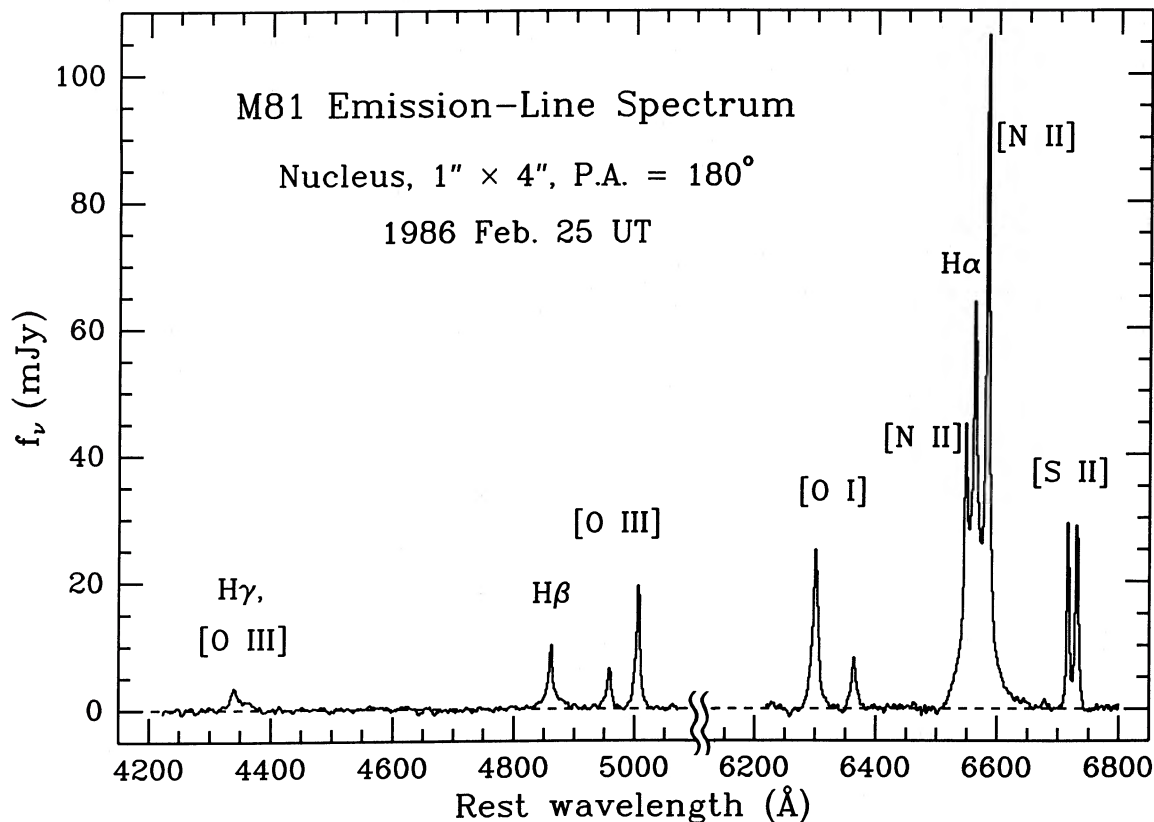


FIG. 3.—The pure emission-line spectra of Figs. 1c and 2c are combined into one composite spectrum. There is a break in the wavelength scale at ~ 5500 . M81 exhibits classical LINER characteristics, with the strengths of [O I], [S II], and [N II] comparable to that of [O III] $\lambda 5007$.

absorption lines are deeper, so the subtraction process is more difficult. The baseline in the net spectrum (Fig. 2c) exhibits some high-frequency oscillations which are probably indicative of slight differences in the detailed spectral characteristics of NGC 4339 and M81. In a future paper, we will critically examine all of the absorption-line galaxies in our spectroscopic survey, constructing linear combinations of templates to minimize the deviations from a flat, smooth baseline.

Despite the presence of these small discrepancies, the subtraction process has immensely improved the appearance of the emission lines in the blue spectrum of M81. In particular, a broad component of H β is readily visible (FWZI ≈ 5800 km s $^{-1}$). PTP claim to have detected this feature, but a glance at their Figure 1c casts doubt on this statement. A corresponding component of H γ is also present in our spectrum. Accurate measurements of its flux and profile are not possible because of strong blending with narrow H γ and [O III] $\lambda 4363$. Note that [O III] $\lambda 4363$ is actually much weaker than one might surmise from a cursory examination of Figure 2a alone; as stressed by FH84, the confusion is produced by a “high point” in the normal stellar continuum at almost the same wavelength. Similar high and low points contaminate the [O III] $\lambda\lambda 4959, 5007$ lines, but not as severely. There is no firm evidence for Mg I $\lambda 4571$, contrary to Table 1 in PTP.

In Figure 3 we show the net emission-line spectrum of M81 on a single ordinate scale, to facilitate visual comparison of the emission lines. The most striking properties are the great strengths of low-ionization lines ([O I], [N II], and [S II]) with respect to [O III] $\lambda 5007$, as well as the wide variety of line widths. Evidently, the narrow-line spectrum is that of a clas-

sical LINER (Heckman 1980), even though the presence of broad H α places M81 into the Seyfert 1 category as well. The possibility that the emission lines in a given object may satisfy the classification criteria of *both* LINERs and Seyfert 1 nuclei has been pointed out previously (FH84; F85; Paper I), but is sometimes not fully appreciated (e.g., Osterbrock 1985).

b) Measurements of Emission Lines

The intensities and widths of all emission lines in Figure 3 were measured interactively. A cursor was used to indicate the endpoints of each line in the spectrum, and the fluxes in all pixels between these endpoints were summed. Points representing the FWHM were also determined. No analytic functions were fitted to the profiles, since the extended wings evident to a greater or lesser extent in all of the emission lines do not have purely Gaussian, Lorentzian, or logarithmic shapes.

A special problem was presented by the [N II] + H α blend: the strong [N II] lines make it very difficult to obtain a reliable measurement of the broad component of H α . Therefore, it was necessary to artificially remove them. Several procedures were attempted. Eventually, we found that of all the emission lines available in our spectra, [S II] $\lambda 6731$ provides the closest match to the observed [N II] profiles in the nucleus of M81. As described in § IVc, a symmetrical, uncontaminated [S II] $\lambda 6731$ profile was synthesized from the red side of [S II] $\lambda 6731$. We could shift its position to any desired point in the spectrum after rebinning the data to a logarithmic wavelength scale, in which each bin represents the same number of km s $^{-1}$. The intensity was also scaled until it matched those of the [N II]

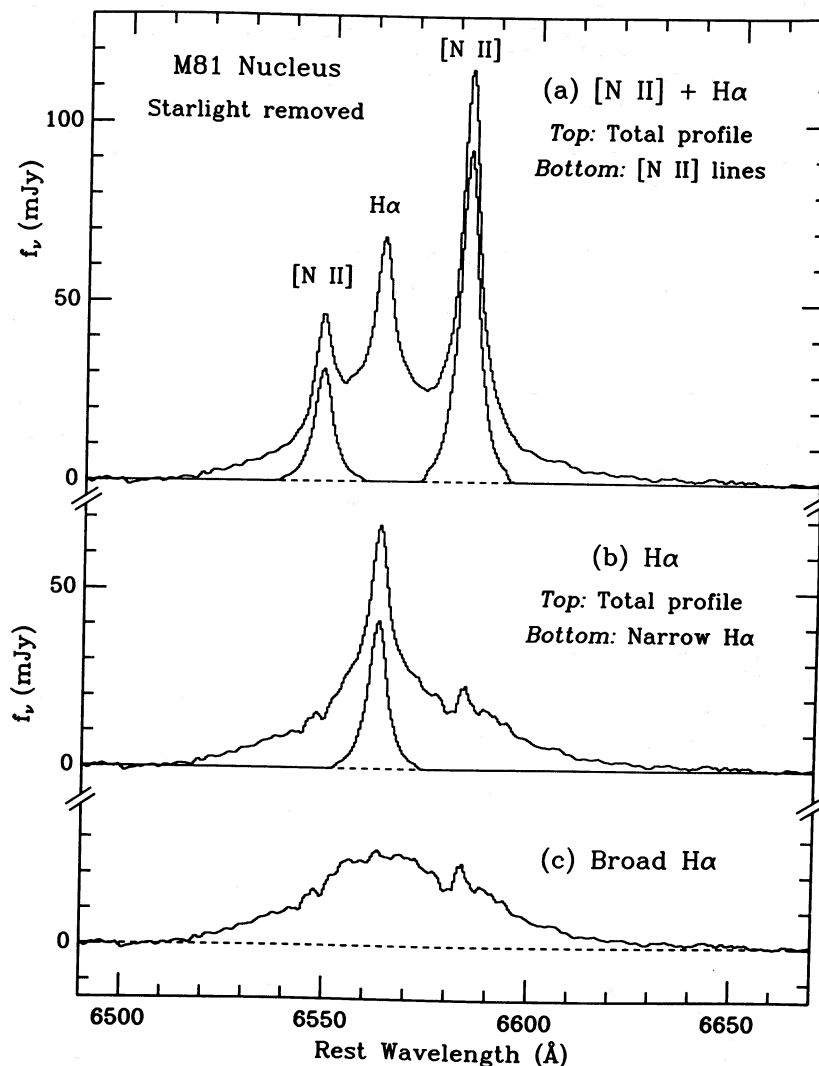


FIG. 4.—(a) The [N II] + H α blend of Fig. 1c is illustrated on an expanded wavelength scale, with each bin corresponding to 22.0012 km s⁻¹. Also shown are suitably scaled versions of the [S II] λ 6731 profile, which closely resembles the profiles of the [N II] lines. (b) Top profile represents H α emission, with the [N II] λ 6548, 6583 lines of (a) excised. A small wiggle is visible at the former position of [N II] λ 6583, and an even less noticeable feature exists at \sim 6548, but otherwise the subtraction is excellent. A scaled [S II] λ 6731 profile is used as a template for the narrow H α line. (c) Subtraction of the narrow H α leaves only the broad component, which can now be measured reliably.

λ 6548, 6583 lines as closely as possible, with the constraint that [N II] λ 6583/[N II] λ 6548 = 2.94, as required by the transition probabilities.

The results are shown in Figure 4a, in which the top profile is that of the [N II] + H α blend and the bottom profiles are those of the synthetic [N II] lines. Figure 4b illustrates the profile of H α after subtraction of the [N II] lines. [S II] λ 6731 does indeed closely resemble the [N II] profiles, although the correspondence is not perfect. A small wiggle in the broad component of H α is evident at \sim 6583 Å, and a similar, but less noticeable, feature exists near 6548 Å. The peaks and valleys of the wiggles, however, roughly cancel each other, leaving the flux of the broad H α unaffected. This is not a coincidence; [S II] λ 6731 was scaled to minimize unrealistic deviations in the final H α profile.

The narrow component of H α (Fig. 4b), which lies on top of the broad base, was eliminated in a similar manner. Figure 4c shows the results, from which precise measurements of the

FWHM (2200 km s⁻¹) and flux (9.52×10^{-13} ergs s⁻¹ cm⁻²) were made. This represents the most detailed attempt to objectively remove the narrow H α and [N II] lines from the nucleus of M81. A similar technique was applied to M81 by Shuder and Osterbrock (1981), and several authors (e.g., Shuder 1980; FH84) have performed such decompositions in other galaxies. PTP measured a flux of 4.5×10^{-13} ergs s⁻¹ cm⁻² for the broad H α , from data of lower quality.

We also used the [S II] λ 6731 profile to subtract narrow H β from the broader component visible in Figure 2c. The [S II] line was artificially broadened with a Gaussian function in order to degrade the spectral resolution to that of the H β region, and its intensity was scaled appropriately. Due to the great strength of absorption lines in this spectral region, the effective S/N ratio in the pure emission-line spectrum is not as high as that near H α . Moreover, the intensity of the H β emission line is much smaller, and H β absorption is particularly troublesome. Nevertheless, the derived profile of the broad H β

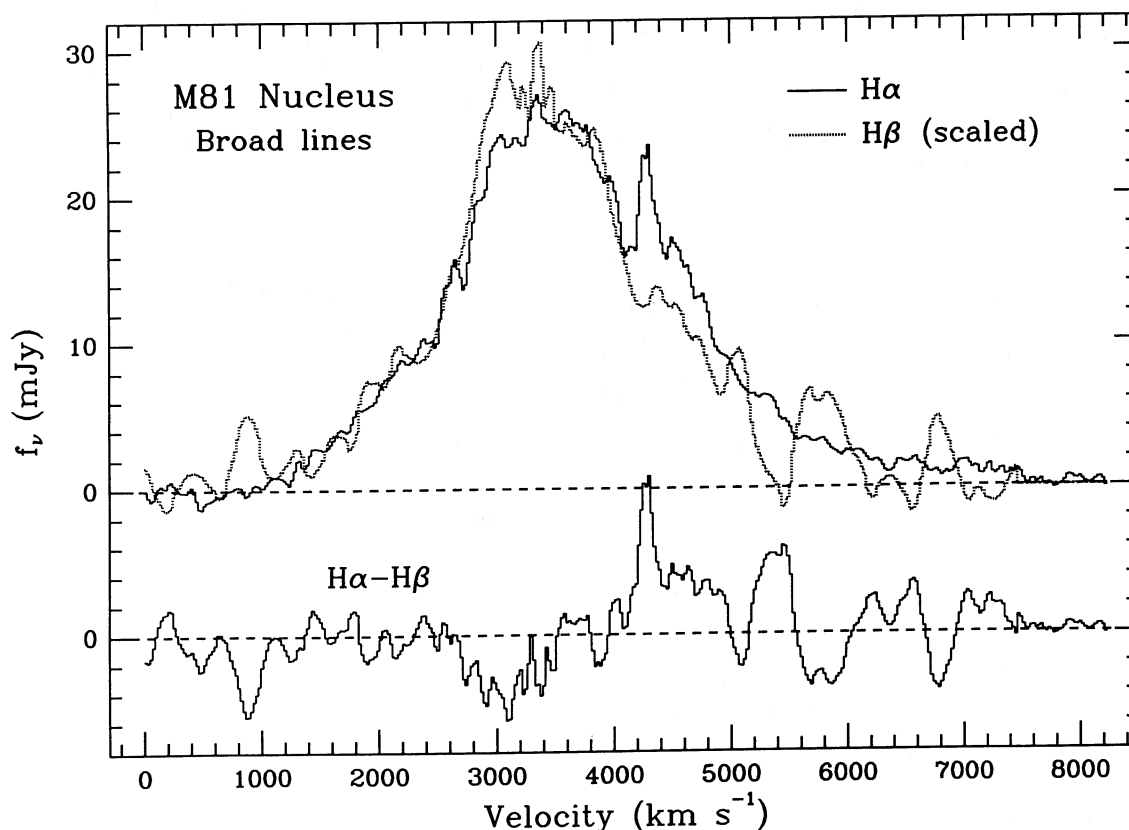


FIG. 5.—The broad $H\alpha$ (from Fig. 4c) and broad $H\beta$ emission lines in M81, free from contamination by starlight and narrow emission lines, are shown on a common velocity scale. The ordinate scale refers to $H\alpha$. Also shown is the difference between the two spectra. Most of the undulations are produced by incompletely removed absorption lines. The narrow feature at $v \approx 4300 \text{ km s}^{-1}$ in $H\alpha$ is located at the former position of $[\text{N II}] \lambda 6583$.

emission is reasonably smooth, and it resembles that of $H\alpha$. This is illustrated in Figure 5, where $H\beta$ has been scaled to the intensity of $H\alpha$. The largest discrepancy appears at the location of the (incompletely) excised $[\text{N II}] \lambda 6583$ line, but the overall agreement is quite good. The FWHM of $H\beta$ is 1800 km s^{-1} , and its flux is $1.4 \times 10^{-13} \text{ ergs s}^{-1} \text{ cm}^{-2}$.

Relative intensities and velocity widths of all emission lines measured in our spectra are listed in Table 2. The equivalent widths and absolute intensities are also given, although it should be emphasized that these quantities are critically dependent on the size and, to some extent, on the shape of the entrance aperture. The broad components of $H\alpha$ and $H\beta$ presumably arise from a spatially unresolved region, despite the rather close distance of M81 ($d \approx 3.3 \text{ Mpc}$; $16 \text{ pc arcsec}^{-1}$). Since an aperture of size $1'' \times 4''$ was used for the measurements, the absolute fluxes of even these lines are expected to have uncertainties of $\gtrsim 20\%$. In fact, preliminary analysis of photometric spectra of M81 and standard stars obtained through a slit of width $4''$ indicates that the true flux of the broad $H\alpha$ line may be $8.5 \times 10^{-13} \text{ ergs s}^{-1} \text{ cm}^{-2}$, $\sim 10\%$ lower than quoted previously. To be consistent with measurements of other emission lines, all of which were made through the small aperture, in this paper we adopt the higher value ($9.5 \times 10^{-13} \text{ ergs s}^{-1} \text{ cm}^{-2}$). The observed luminosity of the broad $H\alpha$ is $1.2 \times 10^{39} \text{ ergs s}^{-1}$, ~ 0.05 that of $H\alpha$ in NGC 4051 (Anderson 1970), the faintest classical Seyfert 1 nucleus (Weedman 1976; Véron 1979).

c) Galactic and Internal Reddening

The relative intensities in Table 2 must be corrected for Galactic reddening, which is taken to be $E_{B-V} \approx 0.038 \text{ mag}$ at the position of M81 (Burstein and Heiles 1984). Reddening internal to M81 should also be removed to increase the validity of conclusions deduced from the line ratios. The only reliable estimate we are able to make is based on the observed and theoretically predicted intensity ratios of $H\alpha$ to $H\beta$; the measurement of $H\gamma$ is too coarse, and crucial parameters necessary for other techniques (e.g., Malkan 1983) are not available. It is now generally agreed (Halpern and Steiner 1983; Ferland and Netzer 1983; Gaskell and Ferland 1984) that X-ray heating leads to an intrinsic $H\alpha/H\beta$ ratio of 3.1 (case B'), rather than ~ 2.85 (case B; Brocklehurst 1971), in the NLRs of AGNs. Since M81 has a Seyfert 1 nucleus, complete with X-rays and other indications of activity, we adopt 3.1 for the intrinsic ratio. The observed value in the NLR, 3.31 (corrected for Galactic reddening), is only slightly larger than this. A color excess $E_{B-V} \approx 0.056 \text{ mag}$ is derived with a standard Whitford (1958) reddening curve (parametrized by Lequeux *et al.* 1979), yielding a total (Galactic plus internal) value of $E_{B-V} \approx 0.094 \text{ mag}$ in the NLR. The corresponding visual extinction is $A_V \approx 3.2E_{B-V} \approx 0.30 \text{ mag}$. All relative intensities of narrow lines were dereddened accordingly.

The situation is much more complex in the broad-line region (BLR), where densities are high ($n_e \gtrsim 10^9 \text{ cm}^{-3}$) and optical

TABLE 2
 EMISSION LINES IN M81

Line ^a	EW ^b (Å)	$F(\lambda)/F(H\beta n)^c$	$I(\lambda)/I(H\beta n)^d$	FWHM ^e (km s ⁻¹)	FWZI ^e (km s ⁻¹)
H γ total	5.10	1.70	1.81
[O III] λ 4363	1.61 ^f	0.55 ^f	0.57 ^f	850 ^f	...
He II λ 4686	<0.31 ^g	<0.15 ^g	<0.15 ^g
H β narrow	1.91	1.00	1.00	218 ^h	1050 ^h
H β broad	5.07	2.65	2.65	1800	5800
[O III] λ 4959	2.93	1.51	1.50	384	2300
[O III] λ 5007	8.16	4.16	4.12	335	2400
[O I] λ 6300 ⁱ	6.99	4.33	3.94	398	2200
[O I] λ 6364	1.85	1.20	1.09	351	1500 ^f
[N II] λ 6548	3.88	2.60	2.33	218 ^h	1050 ^h
H α narrow	5.18	3.46	3.10	218 ^h	1050 ^h
H α broad	26.2	17.5	14.9	2200	6900
[N II] λ 6583	11.5	7.70	6.89	218 ^h	1050 ^h
He I λ 6678	0.26 ^j	0.17 ^j	0.15 ^j	300 ^j	700 ^j
[S II] λ 6716	3.37	2.15	1.91	193	950
[S II] λ 6731	4.08	2.60	2.31	218	1050

^a Line identification, rest wavelength.

^b Equivalent width; strong absorption lines removed.

^c Observed intensity relative to narrow H β . $F(H\beta n) = 5.43 \times 10^{-14}$ ergs s⁻¹ cm⁻².

^d Dereddened: $E_{B-V} = 0.094$ mag (narrow lines), $E_{B-V} = 0.14$ mag (broad lines).

^e Full width at half-maximum, full width near zero intensity.

^f Uncertain measurement ($\sim \pm 40\%$).

^g Upper limit—line not detected.

^h Line profile assumed to be identical to [S II] λ 6731.

ⁱ Possibly contaminated by weak [S III] λ 6312 in red wing.

^j Very uncertain measurement ($\sim \pm 70\%$).

depths to Ly α absorption are exceedingly large. Self-absorption (Netzer 1975) and collisional excitation (e.g., Kwan and Krolik 1981) produce substantial deviations from simple recombination theory. Despite the wide range of possible parameters, in almost all cases these complications *increase* the ratio of H α to H β ; an *upper limit* to the reddening of the BLR can therefore be derived from the observed ratio and 3.1, the case B' value. In the BLR of M81, H α /H $\beta \approx 6.3$ (corrected for Galactic reddening), similar to the high values found in broad-line radio galaxies (Osterbrock, Koski, and Phillips 1976). This gives $E_{B-V} \lesssim 0.60$ mag, or $A_V \lesssim 1.9$ mag. Previous observations of other AGNs indicate that the ionizing continuum emitted by the nucleus is probably reddened far less (see, for example, MacAlpine 1985).

We believe, however, that the BLR of M81 is not heavily reddened, and that the large H α /H β ratio is produced by the extreme conditions in the gas. The observed total strength of the partially blended H γ and [O III] λ 4363 is 1.28×10^{-13} ergs s⁻¹ cm⁻². Of this, we estimate that [O III] λ 4363 contributes at most 4.2×10^{-14} ergs s⁻¹ cm⁻², so $F(H\gamma) \gtrsim 8.6 \times 10^{-14}$ ergs s⁻¹ cm⁻². The expected flux (case B', reddened by $E_{B-V} = 0.094$ mag) of the *narrow* component, 0.45 of the narrow H β , is $\sim 2.44 \times 10^{-14}$ ergs s⁻¹ cm⁻², which means that the flux of the *broad* H γ is $\gtrsim 6.16 \times 10^{-14}$ ergs s⁻¹ cm⁻². Thus, the ratio of broad H γ to H β emission is $\gtrsim 0.43$, very close to the unreddened case B' value of 0.47, and the corresponding broad-line color excess is $E_{B-V} \lesssim 0.2$ mag. If E_{B-V} were equal to 0.60 mag, as formally indicated by the H α /H β intensity ratio, the observed value of H γ /H β would be 0.35 rather than $\gtrsim 0.43$. We adopt $E_{B-V} = 0.1$ mag for the BLR of M81, in addition to the Galactic contribution of $E_{B-V} = 0.038$ mag, but uncertainties in the measurements and the analysis are consistent with a range between 0.00 and 0.25 mag.

The total (Galactic plus internal) color excess derived by PTP and by Bruzual, Peimbert, and Torres-Peimbert (1982;

hereafter referred to as BPTP) for the continuum of M81 is $E_{B-V} = 0.19$ mag, based on a comparison with the continua of M31, M32, and NGC 4472. This is roughly twice the value we deduce from the narrow emission lines. It is possible that the discrepancy is caused primarily by differences in the entrance apertures; we sampled much smaller regions near the nucleus of M81 than did Peimbert and colleagues. In addition, the intrinsic stellar continuum of M81 may differ from those of the galaxies listed above, leading to errors in the derived reddening. Finally, the adopted color excesses of the comparison galaxies may be erroneous, and the extinction curves need not be identical in different objects.

d) The Nonstellar Continuum

The intensity of the broad H β emission line, corrected for extinction ($E_{B-V} = 0.138$ mag), is $\sim 2.3 \times 10^{-13}$ ergs s⁻¹ cm⁻². We may calculate the expected flux of the nonstellar continuum at H β , assuming that this line is produced entirely by recombination. EVS found that a power law of index $\alpha = 1.4$ ($f_\nu \propto \nu^{-\alpha}$) is a good fit to the X-ray continuum of M81. If the *nonstellar* continuum has $\alpha = 1.4$ all the way through optical wavelengths, then the expected equivalent width of broad H β with respect to it should be $W(H\beta) \approx 566 f_\alpha \alpha^{-1} [\lambda(H\beta)/\lambda_0]^{-\alpha} \approx 39 f_a \text{ \AA}$, where f_a is the covering fraction of the broad-line clouds, and $\lambda_0 = 912 \text{ \AA}$ is the Lyman limit. The flux per unit wavelength interval, f_λ , of the nonstellar continuum is simply $I(H\beta)W(H\beta)^{-1}$, or $5.9 \times 10^{-15} f_a^{-1}$ ergs s⁻¹ cm⁻² \AA^{-1} . Suppose $f_a \approx 1$, as in many low-luminosity AGNs (Elvis and Lawrence 1985). If the nonstellar continuum is not reddened at all, then it should account for $\sim 21\%$ of the total observed continuum ($\sim 28 \times 10^{-15}$ ergs s⁻¹ cm⁻² \AA^{-1}) at H β . A more reasonable assumption is that the reddening is comparable to the BLR value, in which case the contribution is $\sim 13\%$, still quite substantial.

This appears not to be the case. Although we are unable to

determine stringent upper limits to the nonstellar continuum with our own data, the shape of the visual continuum is typical of old stellar populations, and the strengths of stellar absorption lines are normal. Moreover, BPTP failed to find a strong nonstellar continuum at *IUE* wavelengths. Finally, extrapolation of the expected optical, nonstellar continuum to X-ray energies results in an X-ray flux much larger than that observed by EVS. The discrepancy is exacerbated if the covering fraction used in calculating the flux of the nonstellar radiation is less than unity.

The problem of accounting for the absolute emission-line strengths of M81 has already been discussed by BPTP, and it is reinforced by the measurements presented here. Perhaps a hot accretion disk ($T \lesssim 8 \times 10^4$ K) produces a large quantity of ionizing radiation in the unobserved gap between the *IUE* and *Einstein* energy ranges. As discussed by Péquignot (1984) and reiterated by F85, this could also account for the observed weakness of He II $\lambda 4686$ relative to H β in objects like M81; there are few photons more energetic than 4 ryd, but a large number between 1 and 4 ryd. If the ionizing continuum were a power law of index 1.4, the predicted ratio of He II $\lambda 4686$ to H β would be $1.99/4^4$ (e.g., Penston and Fosbury 1978), or ~ 0.29 , yet we detect neither broad nor narrow He II $\lambda 4686$ in our spectrum (Fig. 2c; Table 2).

e) The $L_X/L_{H\alpha}$ Ratio

A strong correlation is known to exist between the luminosity of broad Balmer lines and that of the X-ray continuum in QSOs and Seyfert 1 nuclei (e.g., Kriss, Canizares, and Ricker 1980). Elvis, Soltan, and Keel (1984) found that $L_X/L_{H\alpha} = 40 \pm 9$, where L_X is measured in the 2–10 keV band. If the X-ray luminosity from the active nucleus is weak, however, objects such as binary X-ray sources and supernova remnants may dominate the X-ray emission of a galaxy. Therefore, it would be useful to know whether the correlation continues to low-luminosity AGNs. If it does, the dominant mechanism for the production of X-rays may be the same as in QSOs.

The luminosity of the broad H α line in M81 is 1.3×10^{39} ergs s $^{-1}$, corrected for Galactic extinction. This was measured in the spectrum obtained on 1986 February 26 UT, but the analysis in § VIb indicates that the H α line has been constant, or very nearly so, during the past few years. Since the 2–10 keV luminosity was 3×10^{40} ergs s $^{-1}$ in early 1985 (Barr *et al.* 1985), we derive $L_X/L_{H\alpha} \approx 23$ for M81, if $L_{H\alpha}$ was similar in 1986 February and in early 1985. This is 58% of the mean for AGNs quoted by Elvis, Soltan, and Keel (1984), although it is larger than the peak value of ~ 16 . Hence, M81 fits well within the observed range of $L_X/L_{H\alpha}$ among AGNs, and it is certainly not overluminous in X-rays. X-ray binaries and supernova remnants near the nucleus probably contribute little X-ray flux in this object.

In 1978–1979, when M81 was a factor of ~ 3 fainter at X-ray energies than in 1985, $L_X/L_{H\alpha}$ must have been as low as ~ 8 unless the flux of broad H α was also much smaller.³ This is unlikely, in view of the stability of H α described in § VIb. Moreover, the spectrum published by Tonry and Davis (1979) exhibits the broad H α line at a level comparable to what we measured. The small $L_X/L_{H\alpha}$ ratio may partly be due to the

³ Elvis and Van Speybroeck (1982) claim that $L_X/L_{H\alpha} = 83$ for M81 at this time. However, they use L_X in the 0.5–4.5 keV band, which was a factor of 1.7 higher than at 2–10 keV. Also, their adopted luminosity of H α is very low; it was probably derived simply by multiplying the PTP value of $L(H\beta)$ by 2.76 rather than by the observed ratio (6–7).

higher covering fraction, and hence greater emission-line flux, of the broad-line clouds in low-luminosity objects. It could also be related to the inconsistency, outlined in § III d, between the emission-line and continuum luminosities.

IV. PROPERTIES OF THE NARROW EMISSION LINES

a) Line Width versus Critical Density

Figure 6 shows a plot of FWHM against $n_e(\text{crit})$ for six forbidden lines in M81, where $n_e(\text{crit})$ is the critical density for collisional de-excitation of a given line. The general behavior of the lines is very similar to that in the active galaxies NGC 7213, Pictor A, PKS 1718–649, and MR 2251–178 (FH84; F85); broad and narrow lines are those with high and low values of $n_e(\text{crit})$, respectively. Such a trend has also been observed in many Seyfert galaxies by De Robertis and Osterbrock (1984, 1986). A comparison of [O I] $\lambda 6300$ and the [S II] $\lambda \lambda 6716, 6731$ doublet led us to conclude that at least one-third of Heckman's (1980) LINERs exhibit the same phenomenon (Paper I).

As discussed in our previous studies, the interpretation is quite simple. Forbidden lines having different profiles cannot possibly arise from exactly the same clouds of gas. Evidently, some clouds are moving more rapidly than others, and they also preferentially emit certain lines. Since the temperature in the photoionized gas is likely to be roughly homogeneous ($10^4 \lesssim T_e \lesssim 2 \times 10^4$ K), as are the abundances, the most important factor affecting the line strengths is density, n_e . If a wide range of densities is present among the clouds, then those with high n_e will emit lines predominantly associated with high $n_e(\text{crit})$, whereas those with low n_e will produce most of the low $n_e(\text{crit})$ lines. This occurs because the emissivity per unit mass of gas is proportional to the mass if $n_e \lesssim n_e(\text{crit})$, but it is nearly constant if $n_e \gtrsim n_e(\text{crit})$. Thus, different emission lines can act as effective tracers of the density—given a sufficiently broad range of densities, comparable amounts of gas at each density, and a correlation between cloud velocity and density (see, for example, De Robertis and Osterbrock 1986).

Let us make the first-order assumption that the FWHM of an emission line represents the bulk motion of clouds whose density is equal to the critical density for that line (see Wilson and Heckman 1985 for a discussion of this simplification). An unweighted, linear least-squares fit to the data points in Figure 6 shows that $v \propto n^{0.13}$ in M81 (or $v \propto n^{0.10}$ if a weighted fit is performed), with an uncertainty of 0.02–0.03 in the exponent. This relation is similar to those derived in previous studies: the exponent is 0.19 in NGC 7213, 0.10 in Pictor A, and 0.11 in PKS 1718–649. FH84 demonstrate that if the clouds are in Keplerian orbits, and if the luminosity of the ionizing continuum is constant over a dynamical time scale, then $v \propto (nU)^{0.25}$, where the ionization parameter U is the ratio of the number density of ionizing photons to nucleons at the inner face of a cloud. The two-phase model of Krolik, McKee, and Tarter (1981) predicts that U should be roughly constant in the BLRs of QSOs, so that $v \propto n^{0.25}$. In the NLRs of most galaxies we have examined, on the other hand, it appears as though U is not constant (e.g., $U \propto n^{-0.48}$ in M81, if orbits are Keplerian), so the two-phase model may not apply. As discussed below, however, a simpler and more probable interpretation is that the velocities of the clouds decrease more slowly with increasing radial distance than in Keplerian orbits.

The correlation coefficient of the unweighted linear least-squares fit is 0.92, and that of the weighted fit is 0.96, indicating

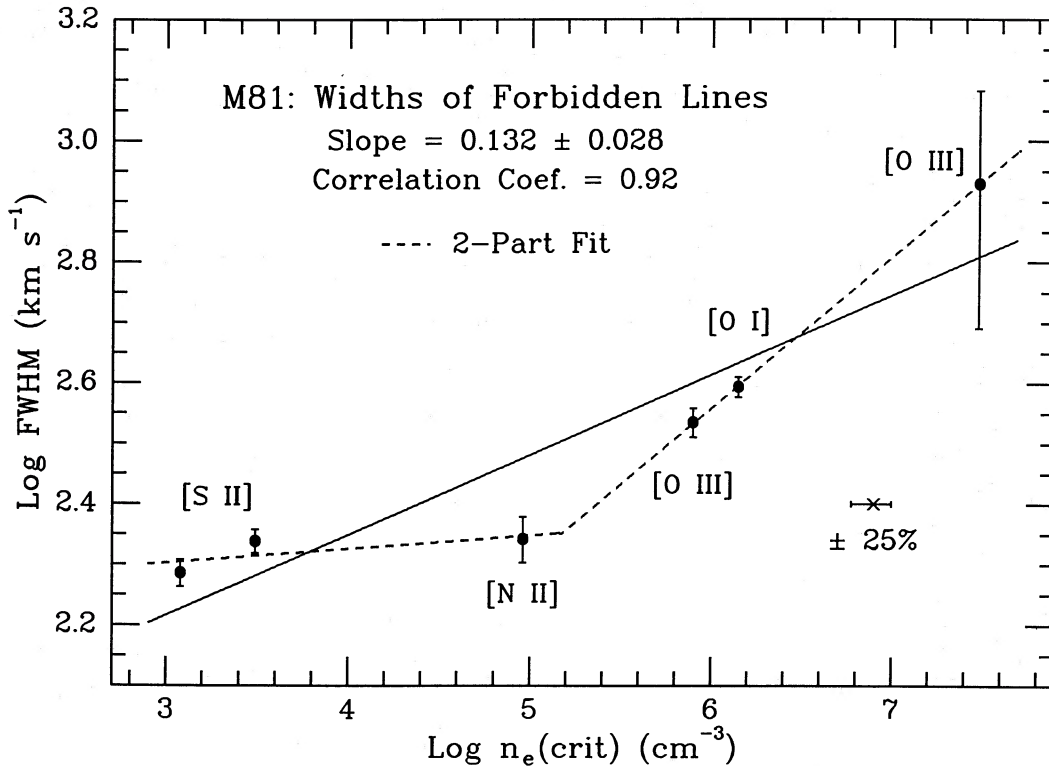


FIG. 6.—The common logarithm of the FWHM of each forbidden line in Figs. 1c and 2c is plotted against that of the corresponding critical density for collisional de-excitation, revealing a highly significant correlation. A horizontal error bar indicates probable uncertainties ($\pm 25\%$) in the theoretically derived values of $n_e(\text{crit})$. The solid line of slope 0.132 ± 0.028 represents the best unweighted, linear least-squares fit to the data; its correlation coefficient is 0.92. A much better fit is obtained with two independent straight lines, as must be the case since there are more free parameters. Quantitatively similar results, however, have been found in other galaxies, suggesting that the two-part fit is physically meaningful.

a probability of over 99% that the correlation is real. Nevertheless, there appear to be systematic deviations in Figure 6 which have also been noticed in other galaxies. Specifically, [N II] $\lambda 6583$ has the same FWHM as the components of the red [S II] doublet, as is the case in NGC 7213 (FH84), Pictor A (F85), and PKS 1718–649 (F85). The [N II] and [S II] lines seem to arise in roughly the same clouds of gas, and these clouds are far enough from the nucleus of the galaxy that they are not part of the velocity field defined by the clouds of higher density. Perhaps the clouds still orbit the nucleus (if orbital motions do indeed dominate the velocities), but in a logarithmic potential, where cloud velocity should be relatively independent of radial distance from the nucleus. Such a potential is produced if the mass density due to stars and dark matter is inversely proportional to r^2 , and dominates that of the central object at the distance of the emission-line clouds. This is quite reasonable if the central mass in M81 is not too large ($M \lesssim 10^6 M_\odot$), as appears to be true (§ Va).

The dotted lines in Figure 6 represent a two-component fit to the width versus $n_e(\text{crit})$ correlation, based on these ideas. In the gravitational infall model of Carroll and Kwan (1983; see also Kwan and Carroll 1982), for example, the [S II] $\lambda\lambda 6716, 6731$ and [N II] $\lambda\lambda 6548, 6583$ lines originate in a low-density reservoir relatively far from the active nucleus. Dense clouds producing [O III] $\lambda\lambda 4959, 5007$, [O III] $\lambda 4363$, and [O I] $\lambda\lambda 6300, 6364$ are at smaller radii. The best unweighted least-squares fit to the latter points yields $v \propto n^{0.25}$, exactly as predicted by the two-phase model of Krolik, McKee, and Tarter (1981). If the [N II] lines are included in the fit, the derived slope decreases slightly, but ~ 0.20 is a firm lower limit.

Of course, we must always keep in mind that it is not really known whether the widths of the lines represent orbital motions, radial flow, or turbulence. By analogy with the BLRs and NLRs as a whole, though, it is natural to assume that the narrow-line clouds having high velocities (and therefore high densities) are closer to the galactic nucleus than low-velocity clouds. Direct evidence for this, to be shown in a subsequent paper, exists in the two-dimensional spectra of a few galaxies such as M81; [O I] $\lambda 6300$ and other lines with high $n_e(\text{crit})$ are confined more closely to the nucleus than the [S II] $\lambda\lambda 6716, 6731$ doublet.

Figure 6 implies the existence of *optically thick* clouds having $n_e \approx 10^6 - 10^{7.5} \text{ cm}^{-3}$. If the high-velocity clouds were optically thin to ionizing radiation, we would not see such broad [O I] $\lambda 6300$ emission. The ionization potentials of O and H are almost identical, so this line is produced only in regions where H^0 and H^+ coexist. Also, as mentioned by FH84 and F85, the presence of several lines from the *same* ionic species but having *different* values of $n_e(\text{crit})$ and dissimilar widths emphasizes the large inhomogeneity in n_e among the clouds of gas. AGNs which lack these two characteristics might be expected to exhibit a better correlation between line width and ionization potential (χ) than between line width and $n_e(\text{crit})$. This is definitely not the case in M81, as demonstrated by Figure 7. The correlation coefficient in the least-squares fit is 0.46, and the [O III] lines have different widths.

b) The [O III] Ratio

The measured, reddening-corrected intensity ratio $R \equiv ([\text{O III}] \lambda 4959 + \lambda 5007)/[\text{O III}] \lambda 4363$ is ~ 9.9 in the

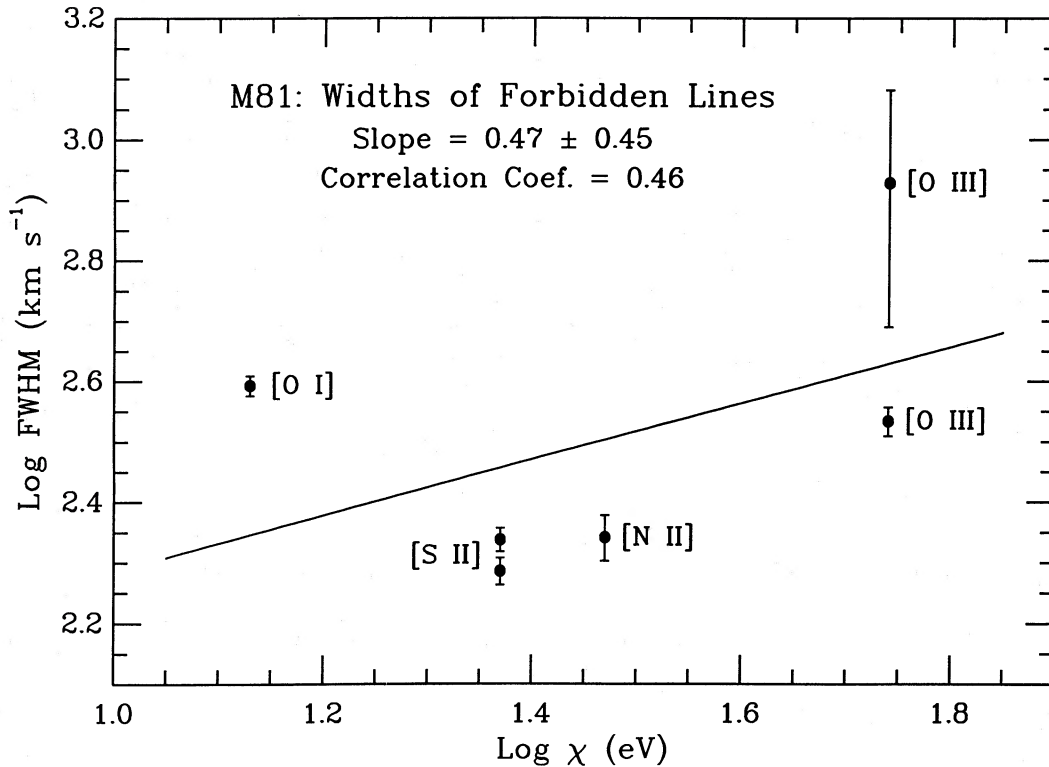


FIG. 7.—A plot of log FWHM against log χ , where χ is the ionization potential of the species under consideration, exhibits much scatter. The unweighted, linear least-squares fit is marginal, with a correlation coefficient of only 0.46 and a poorly constrained slope. This shows that *critical density*, rather than ionization potential, is the fundamental parameter in the narrow-line clouds of M81.

nucleus of M81 (see Table 2), with a possible range of 7–16 due to measurement errors. Adopting an average density of 10^6 cm^{-3} for the O^{++} region, we derive $T_e \approx 19,000 \text{ K}$ from Figure 11 of FH84. Similarly, $n_e \approx 10^7 \text{ cm}^{-3}$ yields $T_e \approx 9000 \text{ K}$. The true temperature is almost certainly between these two limits, but cannot be specified accurately unless R , and hence n_e , are calculated at each point (i.e., velocity) in the line profiles. This is illustrated in Figure 10 of F85. Even then, however, a specific model of the NLR must be adopted in order to determine the amount by which the cores of the lines are contaminated by very dense, high-velocity gas moving transverse to the line of sight. Such a procedure is beyond the scope of this paper. We simply note that the mean temperature found above for the O^{++} region, $\sim 14,000 \text{ K}$, is quite consistent with the idea that the gas is *photoionized* by a nonstellar continuum. Moreover, it is incompatible with shock heating as the dominant ionization mechanism; to produce substantial $[\text{O III}]$ emission, the temperature in a shock-heated gas must be at least $30,000 \text{ K}$.

The integrated intensity ratio $[\text{S II}] \lambda 6731/[\text{S II}] \lambda 6716 \approx 1.21$ implies that $n_e \approx 900 \text{ cm}^{-3}$ if $T_e \approx 10^4 \text{ K}$ in the S^+ region, according to the calculations of Halpern and Filippenko (1988).⁴ This is much lower than the densities in the regions which emit most of the $[\text{O III}]$ emission, as deduced

⁴ The density derived from the graphs of Cantó *et al.* (1980) is 1400 cm^{-3} , but these are based on the older, presumably less accurate, transition probabilities listed by Osterbrock (1974), rather than on the new values published by Zeppen (1982) and used by Halpern and Filippenko (1988). In fact, the results of Cantó *et al.* do not agree with the high-density limit observed in some planetary nebulae (Czyzak, Keyes, and Aller 1986), whereas those of Halpern and Filippenko do.

from the excellent correlation between line width and $n_e(\text{crit})$. Indeed, if we now *assume* that the gas is photoionized, so that $T_e \lesssim 20,000 \text{ K}$ in the regions of interest, the densities derived from the integrated $[\text{S II}]$ measurements cannot possibly be applicable to the $[\text{O III}]$ lines. The argument is essentially that outlined by FH84 for NGC 7213: if $n_e \approx 10^3 \text{ cm}^{-3}$, the low $[\text{O III}]$ ratio (R) observed in M81 is impossible to produce at *any* reasonable temperature ($T_e \lesssim 10^{5.4} \text{ K}$). Instead, a larger density is necessary, and the observed value of R can be achieved even at quite low temperatures.

c) Profiles of the $[\text{S II}]$ Lines

Additional, very powerful, support for this interpretation is found from a careful analysis of the individual $[\text{S II}]$ lines themselves, as mentioned briefly in Papers III and IV. Inspection of Figure 1c reveals that the FWHM of $[\text{S II}] \lambda 6716$ is slightly *less* than that of $[\text{S II}] \lambda 6731$; moreover, the latter appears to have stronger wings than the former. This behavior is visible in each of our high-quality spectra of M81, and its reality cannot be disputed. It is qualitatively similar to the behavior of lines whose critical densities differ by orders of magnitude (e.g., the red $[\text{S II}]$ and $[\text{O I}]$ lines), yet $[\text{S II}] \lambda 6716$ has $n_e(\text{crit}) = 1.2 \times 10^3 \text{ cm}^{-3}$ while $[\text{S II}] \lambda 6731$ has $n_e(\text{crit}) = 3.1 \times 10^3 \text{ cm}^{-3}$. Since the profiles are not identical, different clouds of gas spanning a range of velocities do not have the same $[\text{S II}]$ ratios.

Let us see how severe the effect is in M81. We begin by constructing synthetic profiles of each of the two lines, decomposing the blend in the valley between them. First, the data are rebinned logarithmically, with each bin representing 22.012 km s^{-1} ; this oversamples the original spectra near $\lambda 6725$, in which

each bin was 0.82 \AA ($\sim 37 \text{ km s}^{-1}$). Since other, unblended forbidden lines in the nucleus of M81 are quite symmetric, the individual [S II] lines probably are as well. We also assume that the red half of [S II] $\lambda 6731$ and the blue half of [S II] $\lambda 6716$ are not contaminated by any other lines.

To test the validity of these assumptions, the red half of [S II] $\lambda 6731$ is reflected about an axis which intersects the peak of the profile, and a similar operation is performed on the blue half of [S II] $\lambda 6716$. Figure 8a shows the resulting symmetric [S II] profiles. These are added together in Figure 8b and compared with the original [S II] blend. The agreement is very good.

The bottom portion of Figure 9 shows the intensity ratio [S II] $\lambda 6731$ /[S II] $\lambda 6716$ as a function of position (velocity) in the line profiles, derived from the synthetic profiles constructed above. It increases from 1.0 near the peaks (cores) of the profiles, to 2.4 in the wings at high velocities, consistent with [S II] $\lambda 6731$ being broader than [S II] $\lambda 6716$. The ratio rises monotonically with velocity up to 240 km s^{-1} , and then oscillates slightly for 140 km s^{-1} before increasing once again at $v \approx 400 \text{ km s}^{-1}$. Of course, the relative error is largest at high velocities, since the lines steadily weaken, but its general behavior has been measured reliably.

For simplicity, we approximate the velocity dependence of the [S II] ratio with a quadratic polynomial (Fig. 9), determined by an unweighted least-squares fit to the data. The

tables of Halpern and Filippenko (1988) are then used to assign a density to each measured [S II] ratio as a function of velocity, as shown in the top part of Figure 9. An electron temperature of 10^4 K is assumed throughout. We see that the density of the low-velocity gas is low, whereas that of the rapidly moving gas is high. The derived value of n_e in the line core, $\sim 400 \text{ cm}^{-3}$, is obviously only a lower limit; the [S II] ratio at low velocities must be contaminated by dense, high-velocity gas moving across our line of sight. In the line wings, at $v \gtrsim 440 \text{ km s}^{-1}$, the [S II] ratio formally exceeds the high-density limit (~ 2.3), but a reasonable extrapolation of the curve at lower densities suggests that $n_e \approx 10^{5.8} \text{ cm}^{-3}$. Comparable velocities are implied by the large widths of forbidden lines associated with high $n_e(\text{crit})$, such as [O I] $\lambda 6300$ and [O III] $\lambda 5007$ (Fig. 6).

The [S II] analysis shown here constitutes direct proof that high densities are systematically associated with rapid bulk motions in the NLR of M81. Differences in T_e can produce only small changes in the [S II] ratio, unlike those illustrated in Figure 9, since the upper levels from which the two lines originate are nearly the same. Density, on the other hand, can significantly affect the ratio because $n_e(\text{crit})$ differs by a factor of 2.6 for the two lines. A common assumption when using these lines to determine n_e in ionized gases is that the clouds which produce them all have similar n_e , so that the derived average value is not too heavily influenced by inhomogeneities. This is definitely not true in the nucleus of M81; it exhibits an

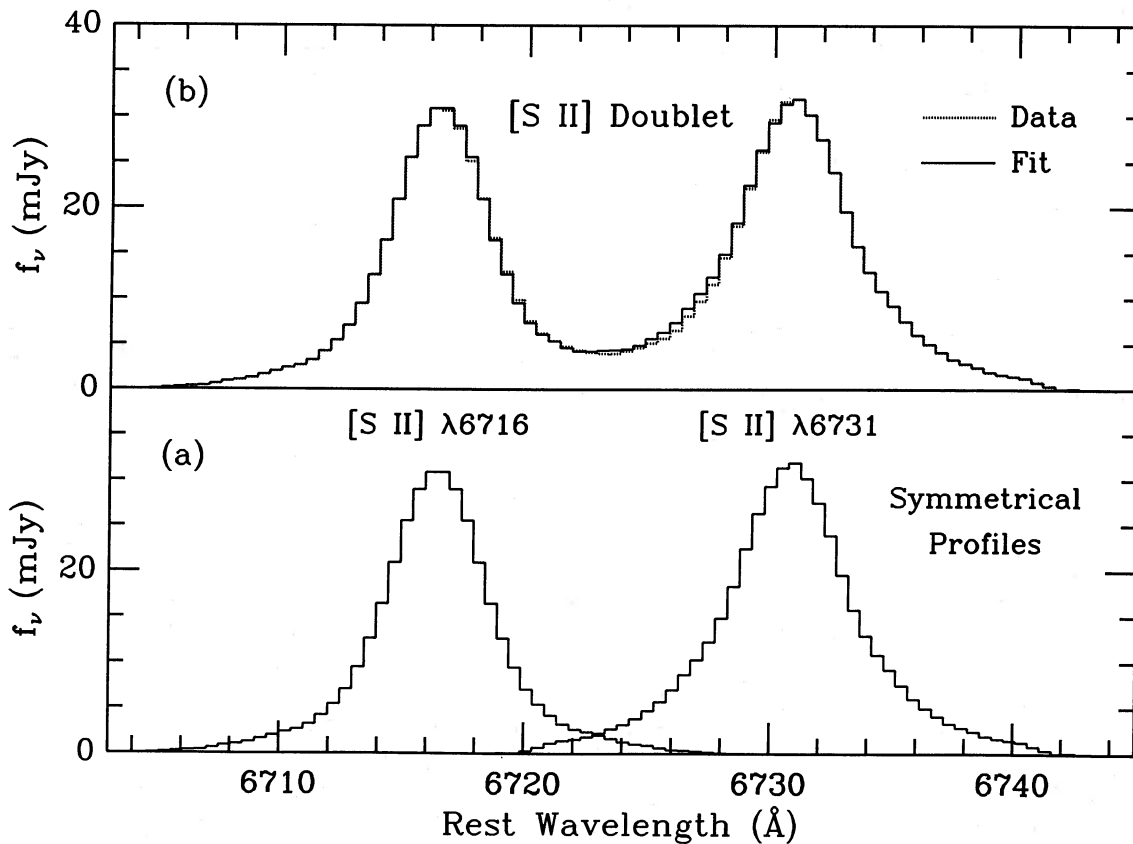


FIG. 8.—(a) Synthetic profiles of [S II] lines in M81 are constructed by reflecting the red half of [S II] $\lambda 6731$ about an axis at 6730.8 \AA and the blue half of [S II] $\lambda 6716$ about an axis at 6716.4 \AA . These two halves are assumed to be uncontaminated by the other member of the [S II] doublet. Each bin corresponds to $22.0012 \text{ km s}^{-1}$. The [S II] $\lambda 6731$ profile appears to be slightly asymmetric because the center of the original line fell mostly on one bin, rather than equally on two adjacent bins, making it necessary to apply a small shift to the spectrum. (b) The sum of the two [S II] profiles (solid line) is a very good approximation to the actual data (dashed line), showing that the assumptions used in the procedure are valid. A small discrepancy is visible in the blue half of [S II] $\lambda 6731$, but it does not affect any of the conclusions.

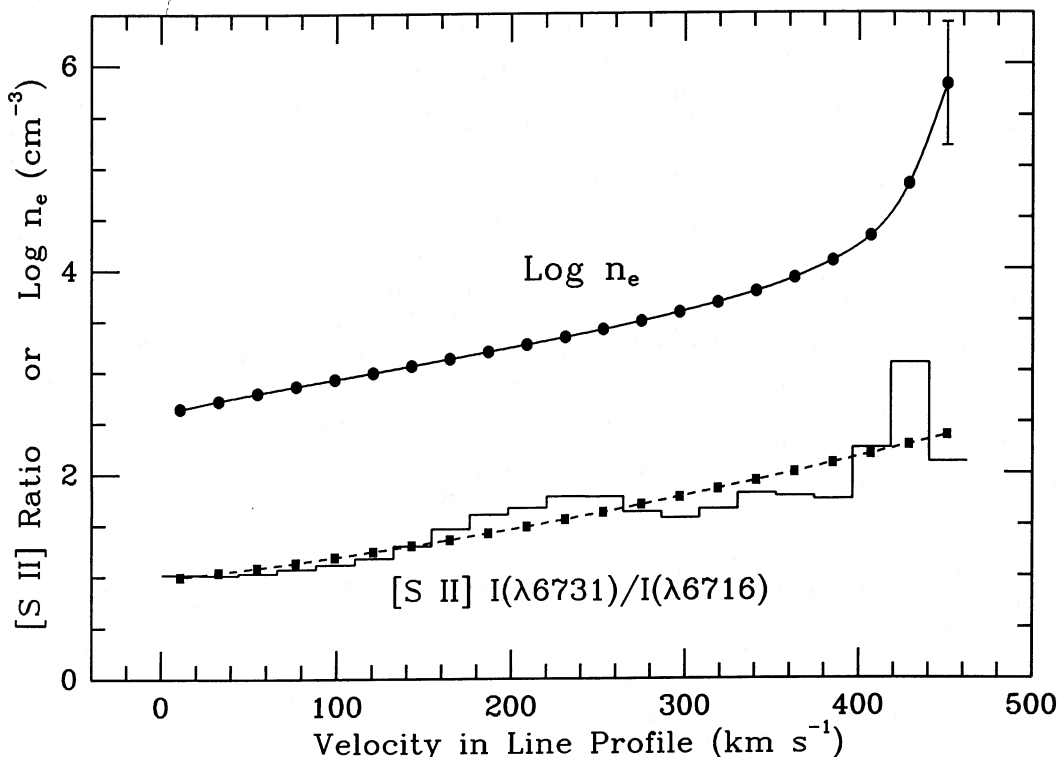


FIG. 9.—The intensity ratio of [S II] $\lambda 6731$ to [S II] $\lambda 6716$ is shown as a function of velocity, or position in the line profile. Symmetric profiles from Fig. 8a are used, and zero velocity is defined as the line peak (core). The measured values are given by the “histogram plot,” with each bin corresponding to $22.0012 \text{ km s}^{-1}$. A quadratic polynomial (dashed line) represents an unweighted least-squares fit to the data. Some of the undulations about this fit are probably real, but here we concentrate only on the overall trend. Filled squares represent the [S II] ratio derived from the quadratic fit at each bin. These values are then used to calculate n_e in the usual way (filled circles). The last point is formally beyond the high-density limit of the [S II] ratio, but extrapolation of the curve leads to $\log n_e \approx 5.8 \pm 0.6$. Note that the derived density in the line core is a lower limit, since the [S II] fluxes must be contaminated by dense gas moving transverse to the line of sight.

extremely sharp gradient of velocity with density, and even closely related lines need not be emitted cospatially. The line profiles demonstrate that a considerable portion of the [S II] $\lambda 6731$ flux is produced by clouds that emit little [S II] $\lambda 6716$. We are currently searching for this effect in other galaxies observed during our survey.

d) The Ionization Mechanism of LINERs

The great strength of [O I] $\lambda 6300$ (Table 2; Fig. 3) and [O II] $\lambda 3727$ (PTP) relative to [O III] $\lambda 5007$ place the nucleus of M81 into the LINER category. Both of the defining criteria established by Heckman (1980), $[\text{O I}]/[\text{O III}] \gtrsim 0.33$ and $[\text{O II}]/[\text{O III}] \gtrsim 1$, are easily satisfied irrespective (within reasonable limits) of the adopted reddening. Based on a comparison of NGC 1052, the prototypical LINER, with observations and theoretical models of shock-heated gas, Koski and Osterbrock (1976) and Fosbury *et al.* (1978) concluded that the emission lines in LINERs also owe their existence to shocks. This hypothesis was adopted shortly thereafter by a number of authors (Ford and Butcher 1979; Heckman 1980; Baldwin, Phillips, and Terlevich 1981). Hence, the spectral similarity of M81 and classical LINERs may imply that NLR gas in the former is also predominantly heated by shocks.

The work of Kent and Sargent (1979), Halpern and Steiner (1983), Ferland and Netzer (1983), Binette (1985), and subsequent authors has shown that the observed spectral characteristics of many LINERs can be understood just as easily with models in which gas is photoionized by a dilute nonstellar continuum, perhaps having a power-law shape with a spectral

index between 1 and 2. If so, it is possible that at least some LINERs are low-luminosity manifestations of the activity common in QSOs and Seyfert nuclei. In particular, M81 is a modest X-ray emitter, and the broad components of H α , H β , and H γ provide a direct link to classical AGNs. A significant fraction of the LINERs in early-type galaxies discussed in Paper I also exhibit broad H α emission, suggesting that they are the faint extension of the AGN luminosity function studied by Huchra and Sargent (1973).

Until recently, one of the main problems with the photoionization calculations seemed to be that the predicted electron temperature is substantially lower than the observed value, derived from measurements of [O III] $\lambda 4363$ and [O III] $\lambda 5007$. Instead, the observed value is much more consistent with shock models if low densities, deduced from the integrated [S II] $\lambda\lambda 6716, 6731$ and [O II] $\lambda\lambda 3726, 3729$ lines, are used. As discussed above, however, the [O III] ratio is incompatible with high T_e if one includes the evidence for high densities in the O^{++} zone.

The existence of such high densities resolves another discrepancy between theory and observations—namely, that the predicted strengths of some low-ionization lines (e.g., [O I] $\lambda 6300$) are substantially lower than those observed. Since the densest clouds are optically thick to ionizing radiation, soft X-rays penetrate deep into their interiors and produce enormous regions in which only $\sim 10\%$ of the H is ionized, leaving O predominantly neutral (Halpern 1982). Under such conditions, enough free electrons exist to collisionally maintain a large population of atoms in the upper level from which [O I]

62300 arises, thereby explaining the great strength of this line in many objects.

Similarly, the wide *range* of densities accounts for many of the other spectral properties in LINERs. In fact, the models of Péquignot (1984) and Stasińska (1984) actually predicted that the range of densities in the NLRs of Seyfert 2 galaxies and LINERs is greater than was previously believed. Their calculations simply could not reproduce the observed intensity ratios of all emission lines when n_e was assumed to be uniform. Even BPTP had remarked that the relative strengths of the narrow lines in M81 could be explained by power-law photoionization, but only if the auroral lines of [O III] and the trans-auroral lines of [S II] originate in regions having $n_e \approx 10^6\text{--}10^7\text{ cm}^{-3}$, much less than the densities ($\sim 10^3\text{ cm}^{-3}$) determined from the nebular lines of [S II] and [O II]. Finally, as mentioned in § III*d*, a reasonable modification of the adopted shape of the ionizing continuum led Péquignot (1984) to resolve the discrepancy between the observed and predicted strengths of He II $\lambda 4686$.

Thus, there are good reasons to believe that the gas in many LINERs is mainly photoionized, rather than heated by shocks, but we need additional concrete examples to see how widespread this phenomenon might be. Indeed, Heckman (1987) shows that LINERs may well constitute a rather heterogeneous class, with classical shocks, winds, and photoionization producing the emission lines in different objects. Moreover, in some of the photoionized cases the ionizing radiation may actually be produced by hot stars, rather than by nonstellar processes in an active nucleus (Terlevich and Melnick 1985). In addition, since clouds of gas are typically moving with speeds of several hundred km s^{-1} , shocks and photoionization could *both* play a significant role in some objects, as in the models of Aldrovandi and Contini (1984).

V. THE CENTRAL MASS OF M81

a) Broad Lines

The observed widths of the broad, permitted emission lines in classical AGNs provided one of the first indications that large masses are involved in these objects (e.g., Woltjer 1959). If the line widths are produced predominantly by the bulk motions ($\sim 0.01c$) of clouds gravitationally bound to the nucleus, then central masses of $10^8\text{--}10^9 M_\odot$ are derived, since many theoretical models agree that the clouds are generally $\sim 0.1\text{--}1$ pc from the source of ionizing radiation.

Dibai (1981*a, b*) emphasized that these are only representative values; it is best to analyze individual objects separately. This has been done by Wandel and Yahil (1985, hereafter WY; see also Wandel 1986). If all of the broad H β emission is produced by recombination under case B conditions, it is shown that the radial distance of typical broad-line clouds can be expressed as

$$r \approx 0.05 \left(\frac{L_{\beta 42}}{n_9 f_a N_{\beta 23}} \right)^{1/2} \text{ pc}, \quad (1)$$

and that the mass enclosed by the BLR (in units of $10^8 M_\odot$) is

$$M_8 \approx 5 \left(\frac{L_{\beta 42}}{n_9 f_a N_{\beta 23}} \right)^{1/2} v_9^2. \quad (2)$$

Here, $L_{\beta 42} = L(\text{H}\beta)/(10^{42}\text{ ergs s}^{-1})$, $n_9 = n/(10^9\text{ cm}^{-3})$, $v_9 = v/(10^9\text{ cm s}^{-1})$, f_a is the cloud covering fraction, and $N_{\beta 23}$ is the column density of the H β -emitting gas in units of 10^{23} cm^{-2} .

Thus, the central mass is expressed in terms of quantities which can be directly observed or estimated. Simplifying assumptions used by WY are $n_9 = 1$, $N_{\beta 23} = 0.3$, and $v_9 \approx \text{FWZI}/4$. Also, $f_a = (L_c/L_1)^{-0.2}$ if $L_c > L_1 = 2 \times 10^{43}\text{ ergs s}^{-1}$, and $f_a = 1$ if $L_c < L_1$, where L_c is the continuum luminosity (νL_ν) at a rest wavelength of 4000 Å (Mushotzky and Ferland 1984; Kinney *et al.* 1985).

Equation (2) yields central masses of $10^6\text{--}10^{10} M_\odot$ for luminous AGNs, in agreement with previous estimates based on ensembles of objects. More remarkable is that the derived mass seems to be directly proportional to the observed luminosity of the optical nonstellar continuum, as if all AGNs emit optical radiation at a constant fraction (~ 0.01 ; WY) of the Eddington limit! As discussed in Paper V, however, this conclusion may be invalid. It is based on many simplifying assumptions, and the observed correlation is mostly a reflection of the fact that both variables are proportional to luminosity. Removal of the common luminosity dependence leaves a rather scattered correlation between line width and continuum luminosity, also found by Joly *et al.* (1985). Its particular form, $v \propto L^{0.2}$, is consistent with several models in which gravity does not dominate, such as radiative acceleration of optically thin clouds ($v \propto L^{0.25}$; see, for example, Mathews and Capriotti 1985). On the other hand, the possibility still remains that the correlation points to gravity as the dominant force on the emission-line clouds, especially in view of the supporting evidence discussed by Wandel and Mushotzky (1986). Using two independent methods, including that of WY, these authors find that $\log(L_B/L_{\text{Edd}}) \approx \log(L_X/L_{\text{Edd}}) = -3 \pm 0.5$.

M81 provides an excellent opportunity to extend the analysis done by WY to AGNs of lower luminosity. The observed flux of the broad component of H β , corrected for Galactic extinction ($E_{B-V} = 0.038$ mag), is $1.63 \times 10^{-13}\text{ ergs s}^{-1}\text{ cm}^{-2}$. This corresponds to a luminosity of $2.1 \times 10^{38}\text{ ergs s}^{-1}$ if the emission is isotropic and extinction in M81 is negligible. Adopting $n_9 = 1$, $f_a = 1$, $N_{\beta 23} = 0.3$, and $v_9 \approx \text{FWZI}/4 \approx 0.15$, we find that $M \approx 3.0 \times 10^5 M_\odot$, or $M \approx 3.5 \times 10^5 M_\odot$ if the BLR is affected by an additional $E_{B-V} \approx 0.1$ mag (§ III*c*). If the high observed intensity ratio of broad H α to H β is mostly due to reddening, then $A_{\text{H}\beta} \approx 2.16$ mag, $L(\text{H}\beta) \approx 1.55 \times 10^{39}\text{ ergs s}^{-1}$, and $M \approx 8.1 \times 10^5 M_\odot$, considerably larger than the values derived above. As a compromise, we will assume that $M \approx 5 \times 10^5 M_\odot$ in much of what follows. For comparison, the total mass of the broad-line gas is $0.007 M_\odot$, distributed among 4×10^5 clouds having $n \approx 10^9\text{ cm}^{-3}$ and $N \approx 3 \times 10^{22}\text{ cm}^{-2}$ (§ VI*b*).

The calculated central mass refers to the volume bounded by the BLR, and it could, in principle, include a substantial contribution from stars. Equation (1), however, shows that $r \approx 0.0022$ pc (extreme values 0.0013–0.0036 pc) for the BLR. This is much smaller than in luminous AGNs, as expected if the broad-line clouds are always produced with the same narrow range of ionization parameters (Krolik, McKee, and Tarter 1981). The volume enclosed by the BLR, $\sim 4.5 \times 10^{-8}\text{ pc}^3$, is exceedingly small. We therefore consider it highly unlikely that a substantial fraction of the derived mass is due to stars. Of course, the size of the BLR has not been directly *measured*; all we really know is that it lies within ~ 0.5 (8 pc) of the nucleus of M81, in which case the entire mass might in fact be attributed to stars.

It is not yet clear whether one should take such estimates seriously. After all, they are based on many assumptions, the most fundamental of which is that the cloud velocities are

induced primarily by gravity. Nevertheless, the low intrinsic luminosity of M81 is quite consistent with the presence of a much smaller black hole (or other central object) than in bright QSOs. Rapid variability at X-ray wavelengths (§ VIa) also suggests that the active nucleus is small in comparison with classical AGNs. A very massive black hole may of course exist in M81, in which case the low luminosity demonstrates that the accretion rate must be extremely sub-Eddington. Similarly, there may be no black hole at all, but we are then faced with the difficulty of explaining the Seyfert 1 activity in M81.

Unfortunately, we lack a direct measurement of the non-stellar continuum luminosity at optical wavelengths; hence, it is impossible to make a direct comparison with $L_{\text{Edd}} = 6.5 \times 10^{43}$ ergs s^{-1} , the expected Eddington luminosity for a black hole of mass $5 \times 10^5 M_{\odot}$. If, however, we adopt the empirically derived relation (Weedman 1985)

$$\mathcal{M}(\lambda 4500) = -2.5 \log [4L(\text{H}\beta)] + 84.70, \quad (3)$$

where $\mathcal{M}(\lambda 4500)$ is the absolute *nonstellar* continuum magnitude of an AGN at a rest wavelength of 4500 Å, it is found that $\mathcal{M}(\lambda 4500) = -12.6$ mag in M81, incredibly faint in comparison with luminous QSOs which have $-30 \lesssim \mathcal{M}(\lambda 4500) \lesssim -23$. The corresponding luminosity, $L(\lambda 4500) \approx 7 \times 10^{40}$ ergs s^{-1} , is $\sim 0.001 L_{\text{Edd}}$ for the mass given above. The approximate agreement with the results of WY and of Wandel and Mushotzky (1986) is not unexpected; $\mathcal{M}(\lambda 4500)$ for M81 was determined from equation (3), which is based on observations of many of the same AGNs used to calibrate the WY relation. Note that if our mass estimate is correct, then M81 could never have been a very bright QSO like 3C 273, which probably requires the presence of an extremely massive black hole.

b) Narrow Lines

Wandel (1986) extends his calculations of the dynamical mass in AGNs to the [O III] lines. He finds that the mass enclosed by the narrow-line clouds is well correlated with the mass within the BLR, and, rather surprisingly, that the two masses are comparable in most objects. If true, this implies that the mass of the central object dominates the kinematics at the radius of the NLR, as well as at the BLR.

If the covering factor, density, and column density of the [O III] producing clouds in M81 are 0.1, 10^6 cm^{-3} , and 10^{20} cm^{-2} , respectively, the observed luminosity of [O III] $\lambda 5007$ yields a radius $r \approx 1.2$ pc, from equation (1) of Wandel and Mushotzky (1986). Similarly, the dynamical mass is $1.9 \times 10^6 M_{\odot}$ within the [O III] region, or ~ 4 times larger than the mass enclosed by the BLR. This suggests that stars dominate the potential in the NLR of M81. If the covering factor were higher, however, the derived mass within the [O III] region would be closer to that of the putative black hole. The observed correlation between $n_{\text{e}}(\text{crit})$ and line width (§ IVa), in fact, implies that the velocity field is largely Keplerian in this region and that stars play an important role only at larger radii.

The radial distance of the clouds producing [O III] $\lambda 5007$, 1.2 pc, corresponds to an angular distance of $\sim 0''.075$. Other emission lines, associated with different critical densities, should be emitted from other regions. The observed line luminosities can be used to determine the relevant radii, as in equation (1), but here we will simply adopt the argument of FH84. If

the lines are produced by gas photoionized by a power-law continuum from the nucleus, then

$$r = d \left(\frac{f_0}{chnU} \right)^{1/2}, \quad (4)$$

where f_0 is the observed flux density of the continuum at the Lyman limit and d is the Earth's distance from the galaxy. We do not see a nonstellar continuum in M81, possibly because it is largely hidden in the 1–4 ryd range (§ IIIa); an equivalent flux will instead be assumed in the form of a power law ($\alpha = 1.4$) sufficient to produce the observed broad H β line. In this case, $f_0 = 1.7$ mJy in M81, so that equation (4) becomes

$$\theta \approx 1.9 \left(\frac{10^3}{n} \right)^{1/2} \left(\frac{10^{-3}}{U} \right)^{1/2} \text{ arcsec}. \quad (5)$$

Thus, if $U \approx 10^{-3}$ is typical of LINERs (Halpern and Steiner 1983), we find that $\theta \approx 0''.06$ for [O III] $\lambda 5007$ ($n \approx 10^6 \text{ cm}^{-3}$), consistent with the value derived earlier. The corresponding angle for clouds emitting low-density ($n \approx 10^3 \text{ cm}^{-3}$) lines such as [S II] $\lambda\lambda 6716, 6731$ is $1''.9$. The different regions may therefore be spatially resolvable with the Hubble Space Telescope.

Finally, we mention that the FWHM of [O III] $\lambda 5007$ is often comparable to that of stellar absorption lines in Seyfert 2 nuclei and LINERs (Wilson and Heckman 1985). A possible interpretation is that the gas and stars sample the same gravitational potential, and that the gas velocities can be attributed mainly to gravity. This approximate equality holds in the nucleus of M81, where the stellar velocity dispersion is $\sim 160 \text{ km s}^{-1}$.

VI. VARIABILITY OF M81

It is now well established that the broad emission lines of AGNs often vary in strength and profile over time periods of weeks, months, and years (see, for example, Tohline and Osterbrock 1976; Oke, Readhead, and Sargent 1980; Yee and Oke 1981; Antonucci and Cohen 1983; Ulrich *et al.* 1984; Peterson *et al.* 1982, 1983, 1984). The time scale of variability is usually shortest, and the fractional amplitude largest, in the low-luminosity nuclei, if one excludes BL Lac objects, optically violently variable (OVV) QSOs, and other AGNs in which radiation is probably beamed toward us. Since the ionization parameter in the BLR is observed to be roughly independent of luminosity among AGNs, this correlation is easily explained; the BLR's radial distance from the nucleus is small in faint objects, and large in bright ones, thereby allowing rapid and significant variability in the former but not in the latter (e.g., Gaskell and Sparke 1986). This can also be seen from equation (1). Variations in the continuum luminosity are understood in a similar fashion. If luminous AGNs generally have black holes of greater mass than faint AGNs, then the regions in which the nonstellar radiation is produced must also be larger.

a) X-Rays

M81 has the least luminous Seyfert 1 nucleus ever measured accurately. If the above discussion is valid, we might expect to see large, rapid variations in the broad H α line, as well as in the (nonstellar) X-ray continuum. Indeed, Barr and Giommi (1985) report that observations with the *EXOSAT Observatory* revealed an increase in the soft X-ray (0.1–4.5 keV) flux by a factor of 5, and in the 2–6 keV flux by a factor of 3, over the *Einstein* measurements obtained in 1978 and 1979. In addition, variability by up to 50% on a time scale of $\lesssim 1$ hr was detected.

Barr *et al.* (1985) and Barr (1986) even mention that at one time the medium-energy (1–6 keV) proportional counters aboard *EXOSAT* showed changes by a factor of 2 in only 600 s, a most dramatic example of rapid variability among AGNs (Barr and Mushotzky 1986). Such rapid changes imply that the volume from which the X-rays originate is very small. If beaming or relativistic expansion do not affect the X-rays in M81, the short time scale of variability implies that the radius of the emitting region is no greater than $c\tau/2 \approx 3 \times 10^{-6}$ pc, where we have taken $\tau \approx 600$ s. Following Wandel and Mushotzky (1986), we assume that the X-rays are emitted ~ 5 Schwarzschild radii from the black hole (Lightman, Giacconi, and Tananbaum 1977) and derive a corresponding mass of $\lesssim 6 \times 10^6 M_{\odot}$. This upper limit is only one order of magnitude higher than the mass we calculated using the formalism of WY (§ Va).

It is important to see whether any sign of variability can be detected at optical wavelengths in M81. The extremely rapid X-ray variations described above should not produce corresponding changes in the permitted emission lines, since the recombination time of the broad-line clouds is ~ 1 hr if their density is 10^9 cm^{-3} . (Note, though, that n may be much higher; see § VIb.) X-ray variations over time scales greater than a few hours or days, on the other hand, might be accompanied by changes in the broad lines if the UV photoionizing continuum is produced by the same mechanism as the X-rays. The radial distance of typical broad-line clouds in M81 is 0.0013–

0.0036 pc, which corresponds to only 1.5–4.3 light days; hence, the BLR can respond very rapidly to changes in the UV continuum. We therefore decided to monitor the broad $H\alpha$ line as frequently as possible.

b) Broad $H\alpha$ Emission

A preliminary comparison of two optical spectra obtained one year apart (Filippenko 1985b) seemed to indicate that the broad component of $H\alpha$ emission had varied by 30%–40% during at least a small portion (1984–1985) of the time period spanned by the X-ray observations. The data, however, were obtained with two different telescopes and spectrographs, and through dissimilar entrance apertures, making the result rather questionable.

Many new spectra of M81 were subsequently taken with the Double Spectrograph on the Hale reflector (Table 1). In most cases the slit was $2''$ wide, and oriented at P.A. = 65° for uniformity. When reducing the data, we used roughly the same regions along the slit to subtract the background sky from M81. We often made a special attempt to monitor the atmospheric seeing by obtaining a two-dimensional spectrum of a neighboring bright star immediately before or after observing M81, and by plotting the resulting spatial profile.

Figure 10 illustrates four representative spectra near $H\alpha$. Two days separate spectra (a) and (b), whereas (c) and (d) were obtained one month earlier and 10 months later, respectively.

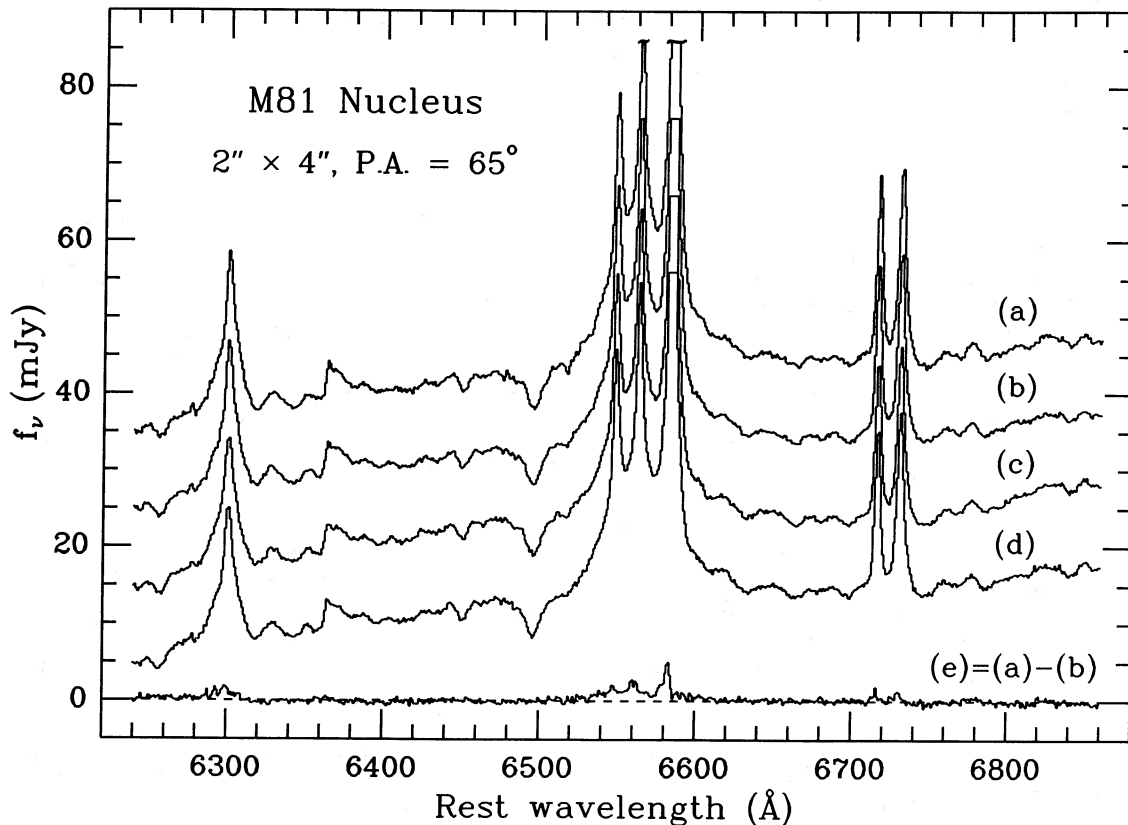


FIG. 10.—Four independent spectra of the nucleus of M81, obtained on (a) 1986 March 27 UT, (b) 1986 March 29 UT, (c) 1986 February 25 UT, and (d) 1987 January 24 UT. The atmospheric seeing disk was estimated to be 0.8 – $1''$, 1 – $1.3''$, 1 – $1.5''$, and $\sim 1.5''$, respectively. Each spectrum has been scaled so that its continuum matches the average flux density of the continuum in (a), which was obtained under photometric conditions. Additive offsets of -10 , -20 , and -30 mJy have been applied to (b), (c), and (d) for clarity. The strong $[\text{N II}] \lambda 6583$ line has been truncated, as has the narrow component of $H\alpha$ in some cases. Spectrum (e) shows (a) minus (b); the residuals can be explained entirely by the slight difference in atmospheric seeing. Comparison of (c) and (a) also reveals no significant discrepancies. The broad $H\alpha$ in (d) is less intense by $\sim 20\%$ than in the other spectra, consistent with the somewhat inferior seeing at the time the spectrum was obtained.

The underlying starlight has not been subtracted. Spectrum (a) was obtained in photometric conditions, and is plotted on an absolute scale. All others were adjusted to make their average continuum flux density in the range $\lambda\lambda 6400\text{--}6500$ equal to that of spectrum (a). Also, in each case we slightly modified the overall shape of the continuum in order to remove broad-band discrepancies caused by atmospheric dispersion, focus variations along the CCD, and other effects. This multiplicative, quadratic polynomial was determined by a least-squares fit to the ratio spectrum between (a) and the other spectrum. Regions containing emission lines were ignored when performing the fit. The final spectra are plotted with additive offsets from (a), for clarity.

The great reproducibility of small features once again emphasizes the high quality of the spectra. Most of the discrepancies are due to imperfect flattening of the two-dimensional data, and to slight spatial variations in the focus, rather than to photon statistics.

In all four spectra the strength and profile of the broad H α emission line are clearly very similar. The difference between (a) and (b) is shown in (e); low-level residual emission is visible at the $\sim 5\%$ level, but this can easily be explained by the slightly inferior atmospheric seeing at the time spectrum (b) was obtained. Since the emission lines are more centrally concentrated than the stellar continuum, their relative slit losses are greater when the seeing degrades, and the continuum scaling procedure does not entirely remedy the situation. Spectrum (c) is also not too different from (a). The broad H α flux in (d) is $\sim 20\%$ weaker than in (a), but once again this is entirely consistent with the significantly worse seeing associated with observation (d).

Together with spectra taken with the same spectrograph in 1984, these data show that the broad component of H α emission has been quite constant over the past 3 yr, at least at the times when observations were obtained. If any variations did in fact occur from early 1984 through early 1987, the H α emission always eventually returned to its nominal level. Although we do not have our own optical spectra from 1978–1979, when the soft X-ray flux was a factor of 5 weaker than in 1985, inspection of the data published by PTP and by Tonry and Davis (1979) suggests that the broad H α line may have been weaker, but not by a comparable amount. The relative constancy of H α is puzzling in view of the substantial X-ray variability of M81, and also in comparison with other low-luminosity AGNs.

It is interesting to consider whether the extremely rapid (0.1–1 hr) X-ray variability in M81 is produced by broad-line clouds moving across our line of sight to a relatively constant source. X-ray spectra of AGNs (Reichert *et al.* 1985; Halpern 1984) and photoionization models of the BLR (Kwan and Krolik 1981; Halpern 1982) indicate that the clouds typically have column densities of $3 \times 10^{22} \text{ cm}^{-2}$; thus, their linear sizes are probably $\sim 3 \times 10^{13} \text{ cm}$, since $n \approx 10^9 \text{ cm}^{-3}$. If the mass of the putative black hole is $5 \times 10^5 M_{\odot}$ (§ Va), and if the X-rays come from a region ~ 10 Schwarzschild radii in diameter, then the broad-line clouds are 20 times larger than the X-ray continuum source. Travelling at 1500 km s^{-1} , it takes ~ 3 hr for a cloud to completely cover the source and ~ 60 hr for the entire cloud to cross over it. This is only marginally consistent with the slowest of the rapid variations. The source would be covered by a cloud most of the time, and the transition to the uncovered state would generally take two or three hours.

Suppose, however, that the broad-line clouds are two orders of magnitude smaller than stated above. This is not unreasonable, in view of the growing evidence that densities in the clouds are actually $\sim 10^{11} \text{ cm}^{-3}$, rather than 10^9 cm^{-3} (Cutri, Rieke, and Lebofsky 1984; Peterson *et al.* 1985; Puetter and Hubbard 1985; Puetter 1986; Gaskell and Sparke 1986). Equation (2) shows that the central mass is then $5 \times 10^4 M_{\odot}$, 0.1 of the previously calculated value. The corresponding size of the X-ray continuum source is $1.5 \times 10^{11} \text{ cm}$, roughly half that of the broad-line clouds. The source can now be covered in 0.28 hr, and the entire eclipse takes only 1.1 hr from first to last contact. Fairly rapid variability may therefore be seen as a cloud flies across our line of sight to the X-ray source. If the source is somewhat larger than we have assumed, Poisson fluctuations in the number of clouds covering it, and in the amount by which they overlap (since f_a is probably ~ 1 in M81), can still lead to rapid apparent variability. A more detailed treatment of this problem will be described in a future paper (Wachter, Strauss, and Filippenko 1988; see also Reichert, Mushotzky, and Holt 1986).

Thus, the intrinsic luminosity of the X-ray continuum in M81 may actually be relatively constant. If so, the rapid variations in X-ray flux seen in the 1–6 keV range should be accompanied by changes in the X-ray spectrum, with the high-energy (≥ 3 keV) X-rays remaining at the same level even when the low-energy absorption is large. Significant fluctuations in the hard X-rays cannot be accommodated by this model and are presumably indicative of intrinsic source variations. Moreover, the broad emission lines are not expected to change rapidly if the X-ray variability is caused predominantly by the motions of clouds across the source. Secular changes in the intrinsic continuum such as those reported by Barr and Giommi (1985), on the other hand, should certainly affect them. (See Paper IV, in which this was misstated slightly.)

VII. SUMMARY

High-quality optical spectra are used to study the nature of the emission-line gas in the low-luminosity Seyfert 1 nucleus of the bright, nearby spiral galaxy M81. A key step in the analysis is the removal of underlying starlight, which heavily contaminates some emission lines. The absorption-line galaxy NGC 4339 is found to provide an excellent fit to the integrated stellar population in the nucleus of M81, and the velocity dispersions of the two objects are nearly equal. Our main results and conclusions are as follows:

1. The nucleus of M81 exhibits a broad component of H α emission (FWZI $\approx 6900 \text{ km s}^{-1}$), in addition to the narrow component (FWZI $\approx 1050 \text{ km s}^{-1}$). This further confirms the discovery of Seyfert 1 characteristics made by Peimbert and Torres-Peimbert (1981) and by Shuder and Osterbrock (1981). After carefully eliminating the narrow [N II] and H α emission lines, we measure the flux and FWHM of the broad H α to be $9.5 \times 10^{-13} \text{ ergs s}^{-1} \text{ cm}^{-2}$ and 2200 km s^{-1} , respectively. Its luminosity, $1.2 \times 10^{39} \text{ ergs s}^{-1}$, is only ~ 0.05 that of the broad H α in the faintest classical Seyfert 1 nucleus, NGC 4051.

2. Our net emission-line spectrum also clearly exhibits, for the first time, a corresponding broad component of H β emission (FWHM $\approx 1800 \text{ km s}^{-1}$). Its profile is quite similar to that of H α . The intensity ratio H α /H β is 6.6, much higher than the expected recombination value of ~ 3 . We use the measured lower limit to the broad H γ emission to argue that Galactic and internal reddening account for only a small fraction of this

discrepancy. Collisional excitation and optical depth effects probably conspire to produce the observed ratio.

3. The intensity ratio $L_X/L_{H\alpha} \approx 23$ in M81 is somewhat lower than the mean of 40 ± 9 found in QSOs and luminous Seyfert 1 nuclei, but higher than the peak value of ~ 16 . Thus, M81 appears to be typical of AGNs in this respect, suggesting that X-ray binaries do not contribute substantially to the X-ray flux in the nuclear regions. The probable absence of a significant nonstellar continuum at optical and UV wavelengths suggests that much of the ionizing continuum may be concentrated in the (unobservable) region between 1 and 4 ryd, rather than in a power law extending from X-ray energies. This also provides better agreement between the observed and predicted ratio of He II $\lambda 4686$ to $H\beta$.

4. From the observed luminosity of the broad $H\beta$ line, we find that the BLR and the ionizing continuum source in M81 are separated by 0.0013–0.0036 pc. If the observed widths of the broad emission lines are produced by clouds gravitationally bound to the nucleus, we calculate a central mass of $3\text{--}8 \times 10^5 M_\odot$. Very little of this can be due to stars enclosed by the BLR, since the BLR's volume is so small. The derived mass is a factor of 10 below the upper limit obtained from the rapid X-ray variability observed by *EXOSAT*.

5. Spectra of $H\alpha$ taken over the past 3 yr show no evidence for variability in flux or profile. This is quite unlike many low-luminosity AGNs, which generally exhibit much more variability than bright QSOs. It is particularly strange in view of the dramatic brightening observed at X-ray energies between 1978 and 1985. The very rapid (~ 600 s) X-ray variability may be due to broad-line clouds crossing our line of sight.

6. Accurate measurements of the narrow emission lines reveal a tight correlation between width and critical density for collisional de-excitation. This has previously been demonstrated in other AGNs. It implies that the NLR is composed of clouds spanning a wide range of electron densities ($10^{2.5} \lesssim n_e \lesssim 10^{7.5} \text{ cm}^{-3}$). Optically thick, dense clouds have the highest bulk motions, and are almost certainly closer to the nucleus than low-density gas. There is some evidence that clouds having $n_e \approx 10^5\text{--}10^{7.5} \text{ cm}^{-3}$ are in pressure equilibrium with a hot intercloud medium, just as the broad-line clouds.

7. We show that in M81 there is a convincing difference between the profiles of [S II] $\lambda 6731$ and [S II] $\lambda 6716$. The ratio of [S II] $\lambda 6731$ to [S II] $\lambda 6716$ increases with velocity in the line profile, providing direct proof that a very steep gradient of

density with velocity exists in the nucleus. These two lines are generally assumed to come from the same clouds of gas, but here this is not the case; much of the [S II] $\lambda 6731$ flux is produced by gas that emits little [S II] $\lambda 6716$.

8. The emission lines in the NLR have intensity ratios typical of Heckman's (1980) LINERs. A color excess (Galactic and internal) of $E_{B-V} \approx 0.094$ mag is derived from the observed $H\alpha/H\beta$ ratio. When full account is taken of the wide range of gas densities, photoionization models involving a nonstellar continuum are easily able to explain the observed relative strengths of emission lines. In particular, the [O III] lines do not indicate high electron temperatures and the great intensity of [O I] $\lambda 6300$ is understood. Shock models, on the other hand, appear to be inconsistent with the data in some respects. The general similarity between M81 and certain other galaxies suggests that the LINERs in most early-type spirals may be genuine AGNs having low intrinsic luminosity.

We thank Juan Carrasco, Mike Doyle, John Henning, Skip Staples, Merle Sweet, Dave Tennant, and Bob Thickett for their nocturnal and diurnal assistance at Palomar Observatory, as well as the Time Allocation Committee for generous quantities of observing time. John Biretta, Robert Deverill, James Fillmore, John Tonry, and the late Peter Young wrote some of the computer programs used to analyze the data. Illuminating discussions with Paul Barr, Jules Halpern, and Amri Wandel are gratefully acknowledged. They also provided useful comments on a preliminary draft of this paper, as did Patrick McCarthy, Joseph Shields, Hyron Spinrad, and Michael Strauss. The work of A. V. F. is partially supported by Cal Space grants CS-21-86 and CS-27-87; that of W. L. W. S., by NSF grant AST 84-16704.

Note added in manuscript, 1987 August 16.—Recently, we learned of several relevant results from a complete spatial and spectral study of M81 at X-ray energies (Fabbiano 1988). The nuclear source appears to be much softer and less absorbed than deduced by EVS, probably because extranuclear objects have been adequately resolved for the first time. If the soft X-ray excess continues to UV energies, there are enough photons to account for the observed emission lines. A hot accretion disk may produce the excess continuum, as discussed in § III d. Using a disk model, Fabbiano (1988) finds a central mass of $10^4\text{--}10^5 M_\odot$ and an accretion rate of $10^{-3}\text{--}10^{-4} M_\odot \text{ yr}^{-1}$, in reasonable agreement with the values derived in § Va from an entirely different approach.

REFERENCES

- Aldrovandi, S. M. V., and Contini, M. 1984, *Astr. Ap.*, **140**, 368.
 Anderson, K. S. 1970, *Ap. J.*, **162**, 743.
 Antonucci, R. R. J., and Cohen, R. D. 1983, *Ap. J.*, **271**, 564.
 Baldwin, J. A., Phillips, M. M., and Terlevich, R. 1981, *Pub. A.S.P.*, **93**, 5.
 Barr, P. 1986, private communication.
 Barr, P., and Giommi, P. 1985, *IAU Circ.*, No. 4044.
 Barr, P., Giommi, P., Wamsteker, W., Gilmozzi, R., and Mushotzky, R. F. 1985, *Bull. A.A.S.*, **17**, 608.
 Barr, P., and Mushotzky, R. F. 1986, *Nature*, **320**, 421.
 Binette, L. 1985, *Astr. Ap.*, **143**, 334.
 Brocklehurst, M. 1971, *M.N.R.A.S.*, **153**, 471.
 Bruzual, A. G., Peimbert, M., and Torres-Peimbert, S. 1982, *Ap. J.*, **260**, 495 (BPTP).
 Burbidge, E. M., and Burbidge, G. R. 1962, *Ap. J.*, **135**, 694.
 ———. 1985, *Ap. J.*, **142**, 634.
 Burstein, D., and Heiles, C. 1984, *Ap. J. Suppl.*, **54**, 33.
 Cantó, J., Elliott, K. H., Meaburn, J., and Theokas, A. C. 1980, *M.N.R.A.S.*, **193**, 911.
 Carroll, T. J., and Kwan, J. 1983, *Ap. J.*, **274**, 113.
 Crane, P. C., Giuffrida, T. S., and Carlson, J. B. 1976, *Ap. J. (Letters)*, **203**, L113.
 Cutri, R. M., Rieke, G. H., and Lebofsky, M. J. 1984, *Ap. J.*, **287**, 566.
 Czyzak, S. J., Keyes, C. D., and Aller, L. H. 1986, *Ap. J. Suppl.*, **61**, 159.
 de Bruyn, A. G., Crane, P. C., Price, R. M., and Carlson, J. B. 1976, *Astr. Ap.*, **46**, 243.
 De Robertis, M. M., and Osterbrock, D. E. 1984, *Ap. J.*, **286**, 171.
 ———. 1986, *Ap. J.*, **301**, 727.
 Dibai, E. A. 1981a, *Soviet Astr.*, **24**, 389.
 ———. 1981b, *Soviet Astr. Letters*, **7**, 248.
 Djorgovski, S., and Spinrad, H. 1983, in *Proc. AAS/OSA Joint Topical Meeting on Information Processing in Astronomy and Optics* (Washington, DC: Optical Society of America), p. ThB2-1.
 Elvis, M., and Lawrence, A. 1985, in *Astrophysics of Active Galaxies and Quasi-Stellar Objects*, ed. J. S. Miller (Mill Valley, CA: University Science Books), p. 289.
 Elvis, M., Soltan, A., and Keel, W. C. 1984, *Ap. J.*, **283**, 479.
 Elvis, M., and Van Spiebroeck, L. 1982, *Ap. J. (Letters)*, **257**, L51 (EVS).
 Fabbiano, G. 1988, *Ap. J.*, submitted.

- Ferland, G. J., and Netzer, H. 1983, *Ap. J.*, **264**, 105.
 Filippenko, A. V. 1982, *Pub. A.S.P.*, **94**, 715.
 ———. 1985a, *Ap. J.*, **289**, 475 (F85).
 ———. 1985b, *IAU Circ.*, No. 4050.
 ———. 1987, in *Supermassive Black Holes*, ed. M. Kafatos (Cambridge: Cambridge University Press), in press (Paper V).
 Filippenko, A. V., and Halpern, J. P. 1984, *Ap. J.*, **285**, 458 (FH84).
 Filippenko, A. V., and Sargent, W. L. W. 1985, *Ap. J. Suppl.*, **57**, 503 (Paper I).
 Fosbury, R. A. E., Mebold, U., Goss, W. M., and Dopita, M. A. 1978, *M.N.R.A.S.*, **183**, 549.
 Gaskell, C. M., and Ferland, G. J. 1984, *Pub. A.S.P.*, **96**, 393.
 Gaskell, C. M., and Sparke, L. 1986, *Ap. J.*, **305**, 175.
 Halpern, J. P. 1982, Ph.D. thesis, Harvard University.
 ———. 1984, *Ap. J.*, **281**, 90.
 Halpern, J. P., and Filippenko, A. V. 1988, in preparation.
 Halpern, J. P., and Steiner, J. E. 1983, *Ap. J. (Letters)*, **269**, L37.
 Heckman, T. M. 1980, *Astr. Ap.*, **87**, 152.
 ———. 1987, in *IAU Symposium 121, Observational Evidence of Activity in Galaxies*, ed. E. Ye. Khachikian, K. J. Fricke, and J. Melnick (Dordrecht: Reidel), p. 421.
 Huchra, J. P., and Sargent, W. L. W. 1973, *Ap. J.*, **186**, 433.
 Joly, M., Collin-Souffrin, S., Masnou, J. L., and Nottale, L. 1985, *Astr. Ap.*, **152**, 282.
 Keel, W. C. 1983, *Ap. J.*, **269**, 466.
 Keel, W. C., and Miller, J. S. 1983, *Ap. J. (Letters)*, **266**, L89.
 Kellermann, K. I., Shaffer, D. B., Pauliny-Toth, I. I. K., Preuss, E., and Witzel, A. 1976, *Ap. J. (Letters)*, **210**, L121.
 Kent, S. M., and Sargent, W. L. W. 1979, *Ap. J.*, **230**, 667.
 Kinney, A. L., Huggins, P. J., Bregman, J. N., and Glassgold, A. E. 1985, *Ap. J.*, **291**, 128.
 Koski, A. T. 1978, *Ap. J.*, **223**, 56.
 Koski, A. T., and Osterbrock, D. E. 1976, *Ap. J. (Letters)*, **203**, L49.
 Kriss, G. A., Canizares, C. R., and Ricker, G. R. 1980, *Ap. J.*, **242**, 492.
 Krolik, J. H., McKee, C. F., and Tarter, C. B. 1981, *Ap. J.*, **249**, 422.
 Kwan, J., and Carroll, T. J. 1982, *Ap. J.*, **261**, 25.
 Kwan, J., and Krolik, J. H. 1981, *Ap. J.*, **250**, 478.
 Lequeux, L., Peimbert, M., Rayo, J. F., Serrano, A., and Torres-Peimbert, S. 1979, *Astr. Ap.*, **80**, 155.
 Lightman, A., Giacconi, R., and Tananbaum, M. 1977, *Ap. J.*, **224**, 375.
 MacAlpine, G. M. 1985, in *Astrophysics of Active Galaxies and Quasi-Stellar Objects*, ed. J. S. Miller (Mill Valley, CA: University Science Books), p. 259.
 Malkan, M. A. 1983, *Ap. J. (Letters)*, **264**, L1.
 Mathews, W. G., and Capriotti, E. R. 1985, in *Astrophysics of Active Galaxies and Quasi-Stellar Objects*, ed. J. S. Miller (Mill Valley, CA: University Science Books), p. 185.
 Münch, G. 1959, *Pub. A.S.P.*, **71**, 101.
 Mushotzky, R., and Ferland, G. J. 1984, *Ap. J.*, **278**, 558.
 Netzer, H. 1975, *M.N.R.A.S.*, **171**, 395.
 Oke, J. B., and Gunn, J. E. 1982, *Pub. A.S.P.*, **94**, 586.
 Oke, J. B., and Gunn, J. E. 1983, *Ap. J.*, **266**, 713.
 Oke, J. B., Readhead, A. C. S., and Sargent, W. L. W. 1980, *Pub. A.S.P.*, **92**, 758.
 Osterbrock, D. E. 1974, *Astrophysics of Gaseous Nebulae* (San Francisco: Freeman).
 ———. 1985, in *Structure and Evolution of Active Galactic Nuclei*, ed. G. Giuricin *et al.* (Dordrecht: Reidel), p. 193.
 Osterbrock, D. E., Koski, A. T., and Phillips, M. M. 1976, *Ap. J.*, **206**, 898.
 Peimbert, M. 1968, *Ap. J.*, **154**, 33.
 Peimbert, M., and Torres-Peimbert, S. 1981, *Ap. J.*, **245**, 845 (PTP).
 Penston, M. V., and Fosbury, R. A. E. 1978, *M.N.R.A.S.*, **183**, 479.
 Péquignot, D. 1984, *Astr. Ap.*, **131**, 159.
 Peterson, B. M., Foltz, C. B., Byard, P. L., and Wagner, R. M. 1982, *Ap. J. Suppl.*, **49**, 469.
 Peterson, B. M., Foltz, C. B., Crenshaw, D. M., Meyers, K. A., and Byard, P. L. 1984, *Ap. J.*, **279**, 529.
 Peterson, B. M., Foltz, C. B., Miller, H. R., Wagner, R. M., Crenshaw, D. M., Meyers, K. A., and Byard, P. L. 1983, *A.J.*, **88**, 926.
 Peterson, B. M., Meyers, K. A., Capriotti, E. R., Foltz, C. B., Wilkes, B. J., and Miller, H. R. 1985, *Ap. J.*, **292**, 164.
 Puetter, R. C. 1986, in *IAU Symposium 119, Quasars*, ed. G. Swarup and V. K. Kapahi (Dordrecht: Reidel), p. 341.
 Puetter, R. C., and Hubbard, E. N. 1985, *Ap. J.*, **295**, 394.
 Reichert, G. A., Mushotzky, R. F., and Holt, S. S. 1986, *Ap. J.*, **303**, 87.
 Reichert, G. A., Mushotzky, R. F., Petre, R., and Holt, S. S. 1985, *Ap. J.*, **296**, 69.
 Rose, J. A., and Tripicco, M. J. 1984, *Ap. J.*, **285**, 55.
 Rothschild, R. E., Mushotzky, R. F., Baity, W. A., Gruber, D. E., Matteson, J. L., and Primini, F. A. 1983, *Ap. J.*, **269**, 423.
 Sandage, A., and Tammann, G. A. 1975, *Ap. J.*, **196**, 313.
 ———. 1981, *A Revised Shapley-Ames Catalog of Bright Galaxies* (Washington, DC: Carnegie Institution of Washington).
 Shuder, J. M. 1980, *Ap. J.*, **240**, 32.
 Shuder, J. M., and Osterbrock, D. E. 1981, *Ap. J.*, **250**, 55.
 Shull, J. M., and McKee, C. F. 1979, *Ap. J.*, **227**, 131.
 Stasińska, G. 1984, *Astr. Ap.*, **135**, 341.
 Terlevich, R., and Melnick, J. 1985, *M.N.R.A.S.*, **213**, 841.
 Tohline, J. E., and Osterbrock, D. E. 1976, *Ap. J. (Letters)*, **210**, L117.
 Tonry, J., and Davis, M. 1979, *A.J.*, **84**, 1511.
 Ulrich, M. H., *et al.* 1984, *M.N.R.A.S.*, **206**, 221; **209**, 479.
 van der Kruit, P. C. 1973, *Astr. Ap.*, **29**, 231.
 Véron, P. 1979, *Astr. Ap.*, **78**, 46.
 Wachter, K. W., Strauss, M. A., and Filippenko, A. V. 1988, *Ap. J.*, submitted.
 Wandel, A. 1986, in *Structure and Evolution of Active Galactic Nuclei*, ed. G. Giuricin *et al.* (Dordrecht: Reidel), p. 727.
 Wandel, A., and Mushotzky, R. F. 1986, *Ap. J. (Letters)*, **306**, L61.
 Wandel, A., and Yahil, A. 1985, *Ap. J. (Letters)*, **295**, L1 (WY).
 Weedman, D. W. 1976, *Ap. J.*, **208**, 30.
 ———. 1985, in *Astrophysics of Active Galaxies and Quasi-Stellar Objects*, ed. J. S. Miller (Mill Valley, CA: University Science Books), p. 497.
 Whitford, A. E. 1958, *A.J.*, **63**, 201.
 Wilson, A. S., and Heckman, T. M. 1985, in *Astrophysics of Active Galaxies and Quasi-Stellar Objects*, ed. J. S. Miller (Mill Valley, CA: University Science Books), p. 39.
 Woltjer, L. 1959, *Ap. J.*, **130**, 38.
 Yee, H. K. C., and Oke, J. B. 1981, *Ap. J.*, **248**, 472.
 Zeppen, C. J. 1982, *M.N.R.A.S.*, **198**, 111.

ALEXEI V. FILIPPENKO: Department of Astronomy, University of California, Berkeley, CA 94720

WALLACE L. W. SARGENT: Department of Astronomy, 105-24 Caltech, Pasadena, CA 91125